Chair of Hydrological Modeling and Water Resources

Albert-Ludwigs-University of Freiburg

Investigation of Flow and Storage Processes at the Shallow Karst Vadose Zone Using Soil Water Isotopes

Björn Henrik Kirste

Examiner: JProf. Dr. Andreas Hartmann

Co-Examiner: Dr. Natalie Orlowski

MSc-Thesis under the guidance of JProf. Dr. Andreas Hartmann

Freiburg i. Br., February 2021

Table of Contents

List of Figures

List of Tables

List of Symbols and Abbreviations

Name	Unit	Symbol
Bulk density	[g cm^{-3}]	ρ_b
Global meteoric water line		GMWL
Inverse of the capillary fringe thickness	[L^{-1}]	α
Leaf area index		LAI
Local meteoric water line		LMWL
Longitudinal dispersivity	[cm]	D_l
Maximum rooting depth	[cm]	RD_{max}
Mean of KGE^{-} values for simulated $\delta^{18}O$ and $\delta^{2}H$	[-]	KGE^{-}_{Iso}
Mean of KGE'_{SM} and KGE^{-}_{Iso}	[-]	SM+Iso
Mean of KGE' values for simulated soil moisture at three measurement depths	[-]	KGE'_{SM}
Modified Kling-Gupta efficiency		KGE'
Mualem-van Genuchten model		MVG
Ratio of stable isotopes ^{2}H and ^{1}H relative to VSMOW	[‰]	$\delta^{18}O$
Ratio of stable isotopes ^{18}O and ^{16}O relative to VSMOW	[‰]	$\delta^{18}O$
Reduced modified Kling-Gupta efficiency		KGE^{-}
Residual soil moisture content	[L^3 L^{-3}]	SM_r
Saturated hydraulic conductivity	[L T^{-1}]	K_s
Saturated soil moisture content	[L^3 L^{-3}]	SM_s
Shape parameter of the hydraulic conductivity function	[-]	m = 1-1/n
Shape parameter of the hydraulic conductivity function	[-]	n
Tortuosity parameter	[-]	l
Vienna Standard Mean Ocean Water		VSMOW

Acknowledgements

First of all, I would like to thank my supervisor JProf. Dr. Andreas Hartmann for providing me with this interesting topic and for his outstanding supervision and encouragements. I am grateful for Dr. Natalie Orlowski being my co-supervisor and for Romane Berthelin introducing me to the topic, providing me with data, and assisting me with the field and laboratory work. In addition, I am very thankful for Stefan Seeger providing and assisting me with the HYDRUS program and for Benjamin Gralher supporting my field work.

Last but not least, I thank my family, my girlfriend Kira, my friends, my flatmates, and my fellow students for supporting me throughout my studies, cheering me up during the time of my thesis, and making my time in Freiburg unforgettable.

Abstract

The shallow karst vadose zone has an important function for dynamics and hydrochemical compositions of karstic groundwater recharge, but its soil hydraulic properties have so far scarcely been investigated. Inverse modeling techniques are a common method to assess these properties. These approaches usually fit simulations to hydrometric data. In this study, the inverse model was expanded by using independent information about the stable isotope composition of the soil pore water depth profile as additional optimization target. The transient unsaturated water flow was simulated by numerically solving the Richards equation with the finite element code of HYDRUS-1D. The transport of stable water isotopes was modeled with the advection-dispersion equation and a modified version of HYDRUS was used, allowing stable water isotope loss during evaporation. The Mualem–van Genuchten parameters, bulk densities, and longitudinal dispersivity parameters were determined for two major soil horizons at two European grassland sites with distinct climatic conditions. The outcomes were compared to the traditional soil hydraulic model approach using only hydrometric data. The study sites were further investigated for soil heterogeneities among grassland and forest areas by analyzing several isotopic depth profiles of soil water. The results showed local heterogeneities of isotopic profiles in the forest areas and low variations in the grassland. For the oceanic climate site in southern England, the traditional model approach accurately reproduced the measured soil moistures. An examination of the simulated isotopic profile, however, showed that the model did not describe the natural transport and storage processes. The hydraulic model concerning soil hydraulic and isotope data also yielded a poor performance. This was due to long transit times of precipitation water through the soil matrix, exceeding the model period. For the humid continental climate site in the Bavarian Northern Limestone Alps, the introduced model approach satisfactorily reproduced the measured soil moisture and isotope values. By depicting not only the soil moisture dynamics but also the transport through the soil matrix, it enabled a more detailed analysis of the soil hydraulic processes. This study shows that water flow and storage processes in the shallow karst vadose zone can be described by a soil hydraulic model. Including soil water stable isotope data improves model realism and allows further insights into soil hydraulic processes.

Keywords: inverse modeling, sensitivity analysis, shallow karst, soil hydraulic parameters estimation, soil water, stable isotopes, vadose zone

Zusammenfassung

Die oberflächennahe ungesättigte Zone in Karstgebieten ist von großer Bedeutung für die dortigen Dynamiken und hydrochemischen Zusammensetzungen des Grundwasserzuflusses. Allerdings sind die bodenhydraulischen Eigenschaften dieser bisher kaum untersucht worden. Zur Erfassung dieser werden häufig inverse Modellierungsansätze verwendet, deren Simulationen üblicherweise an hydrometrische Daten angepasst werden. Der Modellierungsansatz wurde in dieser Studie erweitert, indem unabhängige Informationen über die Konzentrationen stabiler Isotope im Tiefenprofils des Bodenporenwassers als zusätzliches Optimierungsziel verwendet wurden. Der instationäre ungesättigte Wasserfluss wurde durch numerisches Lösen der Richards-Gleichung mit dem Finite-Elemente-Code von HYDRUS-1D simuliert. Der Transport von stabilen Wasserisotopen wurde mit der Advektions-Dispersions-Gleichung modelliert. Dafür wurde eine modifizierte HYDRUS-Version verwendet, die den Verlust stabiler Wasserisotope während der Verdunstung berücksichtigt. Die Mualem-van Genuchten-Parameter, Lagerungsdichten und Parameter für die longitudinale Dispersion wurden für zwei Bodenhorizonte an zwei europäischen Grünlandstandorten mit unterschiedlichen klimatischen Bedingungen bestimmt. Die Ergebnisse wurden mit dem traditionellen Ansatz der bodenhydraulischen Modellierung verglichen, der ausschließlich hydrometrische Daten verwendet. Die Studienstandorte wurden zusätzlich auf Bodenheterogenitäten in Grünland- und Waldgebieten untersucht, indem die Isotopensignaturen des Bodenwassers aus mehreren Tiefenprofilen analysiert wurden. Die Analyse zeigte deutliche lokale Unterschiede der Isotopenprofile in den Waldgebieten und geringe Variationen im Grünland auf. Am Standort mit ozeanischem Klima im südlichen England konnte der traditionelle Modellansatz die gemessenen Bodenfeuchtewerte gut abbilden. Die Betrachtung des simulierten Isotopenprofils wies jedoch darauf hin, dass das Modell die natürlichen Transport- und Speicherprozesse nicht wiedergibt. Das Modell welches sowohl auf bodenhydraulischen Daten als auch auf Isotopendaten basiert, konnte diese Prozesse ebenfalls nicht wiedergeben. Dies ist durch lange Durchgangszeiten des Niederschlagswassers durch die Bodenmatrix zu begründen, die über den Modellzeitraum hinausgingen. Am feucht-kontinentalen Standort in den bayerischen Nördlichen Kalkalpen konnte der in dieser Studie vorgestellte Modellansatz die gemessenen Bodenfeuchte- und Isotopenwerte gut darstellen. Da der Ansatz nicht nur die Bodenfeuchtedynamik sondern auch den Transport durch die Bodenmatrix abbildet, ermöglichte er eine detailliertere Analyse der bodenhydraulischen

Prozesse. Diese Studie zeigt, dass Wasserfluss- und -speicherprozesse in der oberflächennahen ungesättigten Zone von Karstgebieten durch ein bodenhydraulisches Modell beschrieben werden können. Die Einbeziehung von stabilen Isotopendaten des Bodenwassers ermöglicht realistischere Prozessbeschreibungen und detailliertere Einblicke in die bodenhydraulischen Prozesse.

1. Introduction

Karst systems cover 10 – 15 % of global land surface and fully or partially provide water for one fourth of the world population (Ford and Williams, 2013). The process of karstification, however, creates strong morphologic heterogeneities like a porous matrix, fractures, and conduits (Fig. 1). These structures enable fast preferential flow and solute transport and cause a strongly heterogenic groundwater recharge that differs from most other geological areas. An increasing water demand, climate change, and changes in land use are increasingly threatening the quantity and quality of groundwater resources (Wada et al., 2010). Therefore, a more thorough understanding of the processes in karstic areas is needed to better estimate the vulnerability of their groundwater to external changes and to reduce the bias of large-scale hydrological models, which so far do not sufficiently represent karstic areas.

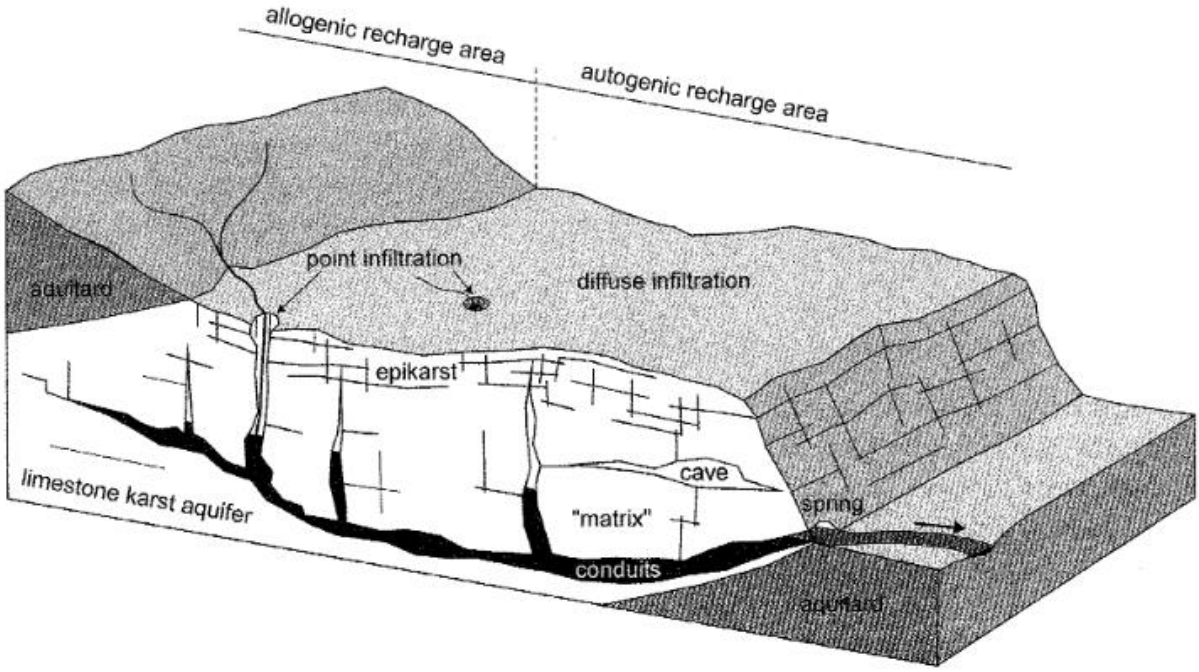

Fig. 1: Schematic illustration of a heterogeneous karst aquifer system (Goldscheider and Drew, 2007).

1.1 State of the Art

1.1.1 Karst Research

The shallow subsurface of karst systems consists of the soil and the epikarst, forming the upper part of the unsaturated zone. It controls various hydrological processes, such as infiltration, storage, and transport processes (Williams, 1983). This area also serves as an important interface between biosphere and karst system (Bakalowicz, 2003).

The epikarst is the zone of superficial weathered carbonate rock and is shaped by rock dissolution (Williams, 1983; Williams, 2008). The dissolution is caused by acids that are a product of the decomposition of organic matter in the soil and epikarst. Acidic water enters into fissures of carbonate rock and dissolves the material, enlarging the fissures rapidly (Dreybrodt, 1990; Benavente et al., 2010). The thickness of the shallow subsurface can vary from less than one meter to up to 15 meters, depending on lithology and geomorphology (Klimchouk, 1995).

Several studies have shown that the epikarst is a main factor for the distribution and quality of karstic recharge water (Aquilina et al., 2006; Trček, 2007; Aley and Kirkland, 2012). Epikarst is highly porous and fractured and can, therefore, store higher amounts of recharge water before larger fractures rapidly redistribute the water to deeper parts of the unsaturated zone.

Above the epikarst, the soil layer also has an important function for the groundwater recharge but only few studies have investigated its role. Perrin et al. (2003) compared the isotopic input signals of infiltrating rain with the isotopic signal of underground and spring water. They concluded that it is necessary to consider both, a soil reservoir and an epikarst reservoir, to describe groundwater recharge and highlighted the importance of the soil zone for infiltration velocity and solute mixing. Charlier et al. (2012) analyzed the recharge input signal and hydrochemical responses in drain and matrix water as well as spring flow to characterize infiltration and transport processes in a karst system. Their results also highlight the importance of soil cover for mixing and transfer of recharge water.

Despite the importance of the upper soil layer and the epikarst for karst water resources, most previous researches focused on karst groundwater. Only few studies investigated and monitored shallow subsurface processes (Berthelin and Hartmann, 2020). Many hydrological processes of the karst vadose zone identified by experimental research have not been incorporated into soil hydraulic models due to problems of model parameter identifiability (Hartmann and Baker, 2017). Most previous studies on the shallow subsurface of karst systems focused only on one

study site and did not compare the dynamics of different systems in different climatic areas (Berthelin and Hartmann, 2020).

1.1.2 Inverse Modeling

Soil physical models are a common tool to describe water flow, groundwater recharge or solute transport in the unsaturated zone (Christiansen et al., 2006). It is challenging, however, to assess the model parameters best describing the soil hydraulic functions (Gribb et al., 2009). Using pedotransfer functions based on grain size distribution of a certain soil or laboratory measurements of the water retention curve or the hydraulic conductivity are common ways to determine soil hydraulic characteristics (Vereecken et al., 2010).

Ries et al. (2015) used one-dimensional water flow models to assess spatial and temporal patterns of soil water percolation in a Mediterranean karst area. They showed how inversely estimated model parameters are effective parameters that describe both preferential and matrix flow. They also concluded that one-dimensional modeling of the soil water balance is a reasonable approach to understand percolation fluxes and subsequent groundwater recharge and that percolation rates strongly depend on soil thickness.

Using a combination of different data types as objective functions in a modeling approach helps to improve parameter identification (Kool et al., 1985; Ritter et al., 2003). Combining hydrometric and hydrochemical data, for example, allows an optimization of both, water flow and solute transport parameters, and reduces the ill-posedness of inverse problems (Mishra and Parker, 1989; Russo et al., 1991).

1.1.3 Using Isotope Data for Modeling

The use of the stable water isotopes deuterium (^{2}H) and oxygen-18 (^{18}O) in the streamflow is one option to include hydrochemical data into the inverse modeling approach and has widely been used to improve the calibration and realism of catchment models (Birkel et al., 2011; Hartmann et al., 2012). If the isotopic composition of infiltrating water varies over time, the water transport within a soil profile can be traced. The time dimension of the tracer is, therefore, contained in the space dimension of the soil (Eichler, 1966). Analyses of pore water stable isotopes have provided useful insights into hydrological processes in the vadose zone of temperate regions, such as infiltration and percolation processes (Darling and Bath, 1988; Thomas et al., 2013) or preferential root water uptake (Gehrels et al., 1998; Brinkmann et al., 2018). These and other studies have shown that the use of stable water isotopes provides several

advantages compared to other naturally or artificially applied tracers. The stable isotopes being part of the water molecule is a major benefit. They can be extracted via root water uptake and, therefore, be used to quantify transpiration. As these isotopes have identical physical properties as water, the composition across a soil profile yields information on several long-term hydrological processes, such as infiltration, evaporation, transpiration, and percolation during both, wet and dry periods. The isotopic composition of stable isotopes can be measured in short time and at high precision (Wassenaar et al., 2008). An analysis of pore water stable isotopes also enables to include dispersivity as transport parameter into inverse modeling approaches, which is not possible with approaches merely using water content or matric potential data (Sprenger et al., 2015b).

Combining soil moisture data with isotope information can help to increase model accuracy and/or reduce the need for measurements (Mattei et al., 2020). Sprenger et al. (2015b) used this approach to determine the most effective way of combining soil moisture and isotope data. They found that the best method with regard to parameter identifiability and model performance is to simultaneously optimize parameters for both measurement objectives. This approach of combining soil moisture and stable isotope data has also been used to determine residence times of soil water and the temporal origin of water taken up by tree roots (Brinkmann et al., 2018).

1.2 Research Objectives

Previous studies highlighted the importance of karstic areas for the global freshwater cycle and water supply. Understanding recharge processes in those areas can help to better estimate and understand large-scale processes and to develop a sustainable management of karstic aquifers. The shallow subsurface of karst systems plays an important role in recharge functioning and water quality but has so far scarcely been investigated. Moreover, most previous studies are limited to a regional scale, not considering different karstic areas with different climatic conditions. The aim of this study is to fill this research gap by parameterizing soil hydraulic properties of the upper part of the shallow subsurface, the vadose soil zone, at three European study sites with distinct climatic conditions. These properties allow to describe and understand recharge and storage processes. The study sites are located in Germany, the United Kingdom and Spain. However, due to the COVID-19 pandemic, the Spanish site could not be accessed and investigated.

The soil hydraulic properties were determined by calibrating an inverse soil hydraulic model. Previous studies showed that the combination of hydrometric and hydrochemical data improves

parameter identification of inverse problems. Determination of pore water stable isotope concentrations allows tracking water particles in the soil for months and can be used to calibrate soil hydraulic properties in the vadose zone. Combining soil moisture and soil water stable isotope data to calibrate a soil hydraulic model has shown to improve model performance. However, this approach has not been tested in karstic areas. In this study, I used the approach of Sprenger et al. (2015b) applying simultaneous parameter optimization with regard to soil moisture and stable isotope concentrations in two distinct karstic areas to answer the following questions.

- Can transport and storage processes at the shallow karst vadose zone be described by a soil hydraulic model?
- Does the inclusion of soil water stable isotope data improve model performance, realism, and parameter identification?
- Are there differences in model performance and parameter identification between the two study sites?

2. Study Sites and Data

For this study, I investigated two karstic sites in Europe, covering distinct climate regions (Fig. 2). The sites are located in the Berchtesgaden National Park (south-east Germany) and on the West Berkshire Downs (southern England). Both sites are part of a soil moisture monitoring network to characterize karstic recharge and evapotranspiration introduced by Berthelin et al. (2020). The locations cover a humid continental and an oceanic climate. To investigate the impact of vegetation on recharge, two plots were selected at each site: one under grassland cover and one under forest. The two plots at each site are chosen at locations with similar slope and exposure. Each plot covers an area of approximately 400 m² and contains 15 soil moisture monitoring profiles, where soil moisture is measured at three different depths.

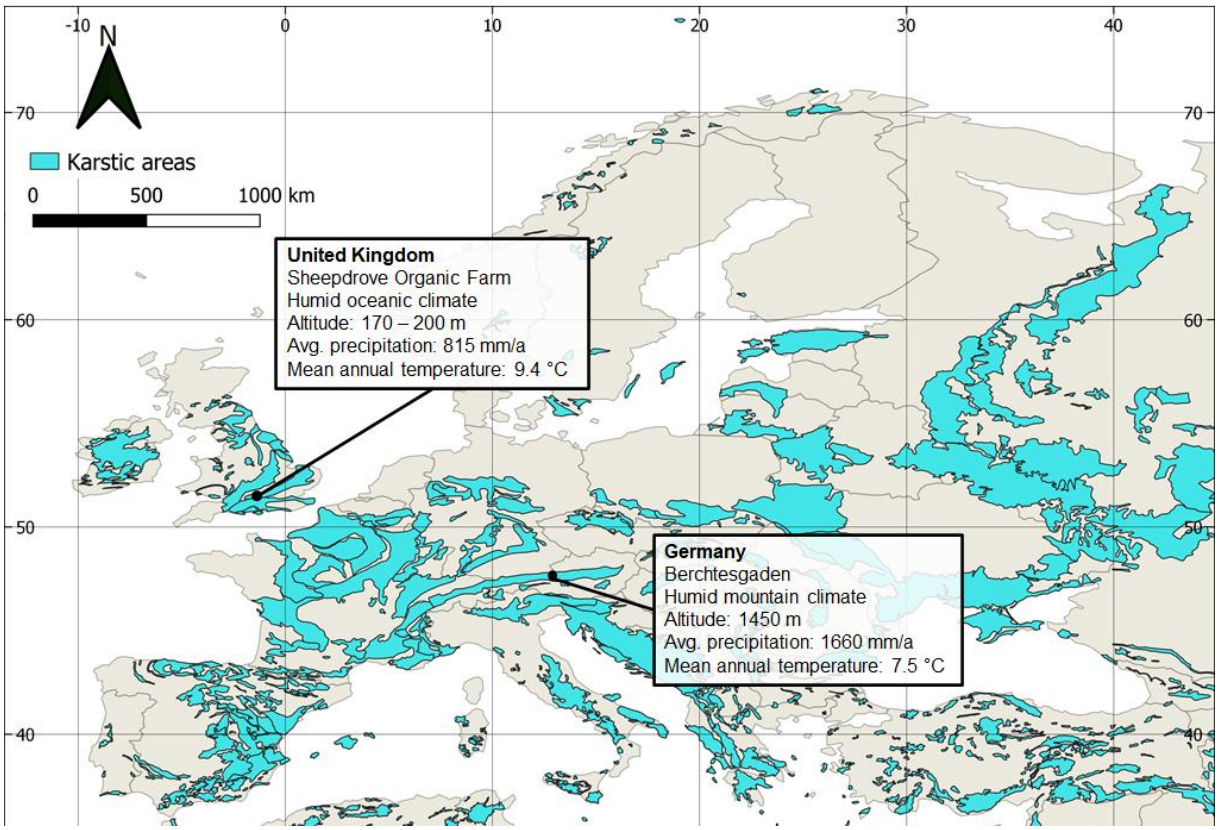

Fig. 2: Karst aquifer map of Europe and locations of the study sites; blue: carbonate rock (Chen et al., 2017).

2.1 German Site

The German site (47.56 °N, 12.96 °E; Fig. 2) is located in the Berchtesgaden National Park in the south-east of Bavaria. The park is part of the Northern Limestone Alps. The climate is classified as warm-summer humid continental climate (Peel et al., 2007), the average temperature is 7.5 °C, and the mean annual precipitation is 1660 mm (Berthelin et al., 2020). The measurement plots are located at an altitude of 1450 m and are covered by snow roughly from November to April or May.

The dominant vegetation in the park is formed by grass, mountain pine, and green alder shrubs (Garvelmann et al., 2017). Triassic Dachstein limestone and Ramsau dolomite are the dominant geological formations next to some Jurassic and Cretaceous rock series. Karstification in form of sinkholes, dry stream, caves, etc., took place since the Alpine thrust exposed the limestone (Berthelin et al., 2020). Several rivers drain three valleys from south to north, contributing to the Danube watershed (Kraller, 2011). The present karst systems contain 330 springs, mostly located at the interface of limestone and dolomite rock (Kraller, 2011). The most common soil types in the national park are Syrosem (35.5%), Cambisol (30.1%), and Podsol (26.7%) (Garvelmann et al., 2017).

The soil characterization at the study site revealed three horizons underneath both plots. The thicknesses of the lower two vary depending on the location. The bedrock underneath consists of limestone. At the grassland plot, the 0 to ~ 15 cm horizon contains a high amount of organic matter and most of the roots (Fig 3 b, c). The ~ 15 to 50 cm horizon has a silty clay texture and contains few roots. The third horizon until ~ 60 cm contains no roots and less clay than the second one. Below 15 cm depth, the soil also contains parts of the limestone bedrock, some of them with > 15 cm diameter, mixed with sand. Apart from grass and weeds, some young pines (< 2 m) grow on the plot.

At the forest plot, the uppermost horizon is ~ 20 cm thick with a high organic content and an abundance of grass roots (in the top 10 cm) and larger roots (diameter < 5 cm; Fig. 3 d, e). The second horizon (~ 20 to 30 cm) has a clay texture and high organic content, which decreases in the coarser third layer (~ 30 to 50 cm). The investigated soil profiles are highly variable, some with layers consisting mostly of rocks with diameters of > 10 cm at various depths. The vegetation consists mostly of grass, ferns, and trees (up to 15 m height), such as spruces and larches. There are some large outcrops on the plot.

Fig. 3: Study site (a) and soil profiles for grassland (b, c) and forest (d, e) at the German site.

2.2 British Site

The UK site (51.53 °N, 1.47 ° W; Fig. 2) is located on the property of the Sheepdrove Organic Farm, at the Berkshire Downs (southern England). The climate is categorized as temperate oceanic climate (Peel et al., 2007), with mean annual minimum and maximum temperature values of 5.4 °C and 14.0 °C, respectively, and an average annual precipitation of 815 mm (Berthelin et al., 2020). The predominant vegetation is composed of meadow and forest with species such as hawthorn bushes, beech trees, cherry trees, and maples (Iwema, 2017 in (Berthelin et al., 2020). The measurement plots are located in the Lambourn catchment and the main geological formation is the Chalk Group of Upper Cretaceous age (Wheater et al., 2007). This formation is the principal aquifer. It is highly permeable and karstified with dry valleys running perpendicular to the Lambourn River and with a groundwater table at tens of meters depth (Wheater et al., 2007; Rahman and Rosolem, 2017).

Soil characterization in the field showed that the soil under the grassland area can be divided into two horizons (Fig. 4 b, c). The upper one (0 to ~ 10 cm depth) contains most of the roots and has a silty texture. The lower horizon (~ 10 cm to various depths) is of silty texture and contains few roots, pieces of chalk (diameter < 2 cm), and flintstones (diameter > 6 cm). The abundance of roots and flintstones decreases with depth while the number of chalk stones and the soil density increase. The bedrock consists of white chalk and appears at a depth of 30 to 60 cm with a continuous transition between soil and chalk.

The soil of the forest plot is covered by a 5 to 10 cm thick layer of organic litter (Fig. 4 c, d). The underlying horizon reaches from ~ 5 cm to a soft calk layer at 10 to 35 cm depth. Small roots were found mostly in the upper 10 cm and larger roots across the entire soil profile. There are some flintstones (diameter > 6 cm) and pieces of chalk (diameter < 2 cm). The latter increase with depth, forming a continuous transition between soil and chalk layer. Laboratory soil texture analyses show fractions of 24 % sand, 47 % silt, and 39 % clay (Berthelin et al., 2020).

Fig. 4: Study site and soil profiles for grassland (a, b, c) and forest (d, e, f) at the British site.

2.3 Data Availability

The soil hydraulic model requires data on climatic conditions, soil moisture, concentration of stable isotopes in precipitation and soil water, vegetation parameters, latitude, and altitude of the study sites to calculate the water and isotope transport. The availability of these data varied among the profiles (Tab. 1).

The climate data include daily values of precipitation quantity, minimum and maximum temperature, relative humidity, windspeed, and global radiation. At the German site, these data were obtained from a weather station in the direct vicinity of the soil moisture plots and provided by the research and monitoring unit of the Berchtesgaden national park service. The climate data for the British site were recorded by a weather station a few meters from the grassland plot and provided by Rafael Rosolem of the University of Bristol. These data do not include windspeed or global radiation measurements. Those values were obtained from the 35 km distant weather station Lyneham of the British Met Office (Met Office, 2006a, 2006b).

Soil moisture data at both study sites was obtained from previously installed sensors (Berthelin et al., 2020). This monitoring network includes 30 soil moisture profiles at each study site, 15 at the grassland and at the forest plot, respectively. At each profile, three SMT 100 sensors (TRUEBNER GmbH, Neustadt an der Weinstraße, Germany) have been installed, one each at 5 and 10 cm depth and at the maximum depth directly above the bedrock. Measurements of these sensors are based on the travel time of an electric signal to determine the dielectric constant of the soil. The sensors measured at a 15-minute interval and the data was collected with two TrueLog100 data loggers (TRUEBNER GmbH, Neustadt an der Weinstraße, Germany). The sensors have not been calibrated and, therefore, do not display the correct absolute values but rather the temporal dynamics of the soil moisture. Due to hardware problems or battery failure, the recorded soil moisture data did not cover the entire sampling period.

The isotopic composition of the soil water was determined by means of soil samples taken at the study sites (see sections 3.1 and 3.2). For the simulations, I used data of the 2019 measurement campaign, carried out by Romane Berthelin. One soil water isotope profile and one nearby soil moisture profile with a consecutive measurement period were selected as data source for the simulations. The stable isotopes compositions of precipitation water for the German site were obtained from a station in Golling, Austria (Umweltbundesamt, 2020). This station is located 16 km from the study site and at an altitude of 476 m a.s.l., almost 1000 m lower than the study site. The precipitation isotopic composition at the British site was obtained from the 25 km distant Global Network of Isotopes in Precipitation station in Wallingford (data not published).

Tab. 1: Available data for the fitting targets of the inverse model.

		German Site	British site
Climate data	Sampling period (interval)	17 October 2013 – 18 October 2020 (10 min)	1 July 2015 – 17 November 2020 (1 h)
Soil moisture data	Sampling period (interval)	15 Jun 2018 – 14 Sep 2020 (15 min)	22 Jun 2018 – 19 Jul 2020 (15 min)
	Sampling depths [cm]	5, 10, max[a]	5, 10, max[a]
Isotope profiles sampling		4 Jun 2019 and 14-15 Sep 2020	16 May 2019 and 25-26 Aug 2020
Precipitation isotopes	Sampling period (interval)	October 2013 – January 2020 (1 month)	January 2016 – June 2020 (1 month)
Model period		4 March 2019 – 4 September 2019	16 February 2020 – 16 August 2020

[a] maximum depth, directly above the bedrock

3. Methodology

3.1 Field Work and Measurements

Two sampling campaigns were carried out, one each at the British site (August 25 - 26, 2020) and at the German site (September 14 - 15, 2020). The purpose was to collect soil samples for subsequent analysis of stable water isotopes in the soil water. Three soil cores at each plot, i.e. grassland and forest, were extracted using a percussion gouge of one meter length and 50 mm diameter and an electric percussion hammer (Fig. 4 c, f). After extraction, the cores were shielded from direct sunlight and rain to prevent evaporation and contamination with rainwater. The soil structure was examined and the core was divided into samples of 5 cm thickness each, up to a depth of 60 cm, totaling to twelve samples per core and 36 samples per plot. In case of compaction, i.e. if the extracted soil core was shorter than the depth of the borehole, this compaction was assumed to be equally distributed across the profile and the thicknesses of the samples were adjusted proportionally. The samples had a minimum weight of 50 g, which is sufficient for isotopic analysis in the laboratory. Each sample was filled into an airtight sampling bag and as much air as possible was expelled before sealing the bag, in order to avoid interactions between soil water and air. To avoid microbial activity, the bags were stored cool until the laboratory analysis was performed.

3.2 Laboratory Work

The analysis of the soil water isotopic composition was carried out using the equilibrium method based on the equilibrium of liquid and gaseous H_2O (Wassenaar et al., 2008). The sample bags were analyzed within one week after the field campaign, as after ten days of storage water losses and isotopic enrichment due to evaporation can occur (Hendry et al., 2015). This method allows to determine $\delta^{18}O$, the ratio of oxygen-18 (^{18}O) and oxygen-16 (^{16}O) isotopes, and $\delta^{2}H$, the ratio of deuterium (^{2}H) and hydrogen-1 (^{1}H), by measuring the stable isotopic composition of pore water vapor in the sample bag. For the direct water vapor equilibration method, the bags were filled with dry air, thermo-welded for airtight closure, and stored at constant room temperature for an equilibrium time of 15 to 48 hours (Sprenger et al., 2015a). For the analysis of water vapor stable isotopes, a WS-CRDS spectrometer (Wavelength-Scanned Cavity Ring Down Spectroscopy, Picarro, Inc., Santa Clara, CA, USA) was used. Three reference samples with known concentrations of ^{18}O and ^{2}H were analyzed at the beginning, in the middle, and at the end of the measurement campaign and used for calibration

(Sprenger et al., 2015a). The water vapor isotopic composition was determined by penetrating the sample bags with a needle attached to the continuous flow spectrometer, which performed the measurement. Using the reference samples, the values displayed by the spectrometer were calibrated against the Vienna Standard Mean Ocean Water (VSMOW). The measurement accuracy, given as the average range of repeated measurements of these standards at the day of measurement, was 0.70 ‰ for ^{18}O and 2.48 ‰ for ^{2}H.

3.3 Modeling

The modeling of water flow and isotope transport was carried out for the grassland plot at both study sites. The data of a neighboring pair of soil moisture and stable isotope was used for model calibration.

3.3.1 Water Flow

To simulate the transient water flow within the unsaturated soil profiles, a modified version of HYDRUS-1D (Šimůnek et al., 2008; Stumpp et al., 2012) was used to numerically solve the Richards equation. The Mualem-van Genuchten model (MVG; van Genuchten (1980)) was applied to parameterize the water retention and the unsaturated hydraulic conductivity function. The parameters to describe these functions are the residual and saturated soil moisture (SM_r [-] and SM_s [-], respectively), the inverse of the capillary fringe thickness (α [L^{-1}]), two shape parameters (n [-], and m [-], with $m = 1- 1/n$), the saturated hydraulic conductivity (K_s [$L\ T^{-1}$]), and a tortuosity parameter (l [-]). Some parameters were fixed to reduce the number of free parameters. The tortuosity parameter l was set to 0.5, in accordance to Mualem (1976). For the German site, SM_r was set to the lowest measured soil moisture value, and for the British site, SM_s was set to the highest measured soil moisture value.

A root water uptake model (Feddes et al., 1978) that describes the reduction of the potential water uptake by a dimensionless trapezoidal stress response function was introduced as sink term for the Richards equation. These restrictions of root water uptake are defined by pressure heads above and below which the plants experience oxygen or water stress, respectively. The parameter set for pasture (Wesseling, 1991) was used to describe these pressure heads for both sites. The model of Jarvis (1989) was used to estimate the root distribution.

The potential evapotranspiration was estimated with the Hargreaves formula as a function of global radiation and daily maximum and minimum air temperature (Hargreaves, 1973). According to Beer's law (Ritchie, 1972), the potential evapotranspiration was divided into

potential evaporation and potential transpiration. The leaf area index (LAI) was set to three for both grassland sites (Byrne et al., 2005). The interception of precipitation water was estimated as a function of precipitation, LAI, and an empirical constant which was set to 0.55 mm, resulting in a maximum interception of 1.65 mm.

For the German site, the Energy balance Snow Cover Integrated Model (ESCIMO; Strasser and Marke (2010)) was included. This allows precipitation water to cumulate as a snow cover and later infiltrate as meltwater or evaporate. The isotopic composition of the meltwater is assumed to be the weighted mean of all precipitation water that contributed to it.

3.3.2 Isotope Transport

The standard version of HYDRUS-1D is not designed to simulate the transport of stable water isotopes. Therefore, simulations were run with a modified isotope-enabled version that also simulates the transport of ^{16}O and ^{2}H as solute transport. This version of HYDRUS-1D allows solute losses caused by evaporation and thereby prevents an accumulation of the stable water isotopes at the upper boundary. It does not account for fractionation processes. The δ notation relative to the Vienna Standard Mean Ocean Water (VSMOV) and an offset value were used for the calculations of the isotopic compositions.

The transport of ^{18}O and ^{2}H was calculated within the HYDRUS code by using the advection–dispersion model. This model is widely used to predict solute transport in soils under field conditions (Vanderborght and Vereecken, 2007). In this model, the mean water flux accounts for the advective part of the equation, while hydrochemical dispersion and molecular diffusion account for the dispersion term.

All profiles were discretized into 101 nodes. To enhance the model stability, the node density at the top was higher than at the bottom. The profiles were also divided into two horizons, with the upper horizon from 0 to 14 cm depth, the lower horizon from 16 to 100 cm depth, and a linear transition of the soil properties between the profiles. The depth of the simulated profiles was 100 cm.

3.3.3 Initial Boundary Conditions

The site-specific initial $\delta^{18}O$ and $\delta^{2}H$ values were defined by a weighted average of the precipitation concentration. The initial soil water contents were set to 1 for the German site, assuming a fully saturated soil because of the snow melt in spring, and 0.25 for the British site. The upper boundary condition was defined as Cauchy boundary condition with variable

atmospheric conditions governing the input of water and stable isotopes through precipitation and their loss caused by evaporation. The modified HYDRUS code allows that evaporation only influences the amount of water but not its isotopic composition. The lower boundary was set to zero-gradient with free drainage of water and solutes. Including a warm-up period of one year did not improve the model performance and yielded worse efficiency values at the German site. It was, therefore, omitted.

3.3.4 Parameter Optimization and Sensitivity

Six parameters were optimized for both horizons of the soil profiles to simulate the water and solute transport in the unsaturated zone. These include the four parameters SM_r or SM_s, α, n, and K_s as the MVG parameters describing the water retention and hydraulic conductivity characteristics; as well as the longitudinal dispersion coefficient D_l and the bulk density ρ_b, which are both parameters of the solute transport model. In addition, the maximum root depth was subject to optimization, totaling to 13 parameters for each soil profile. The ranges of the parameter spaces were based on expert knowledge and are listed in Tab. 2.

To find the best parameter set, random combinations of parameters were picked using a Monte Carlo algorithm (Metropolis and Ulam, 1949). At each realization, the thirteen parameters were randomly picked from within the pre-defined range, inserted into the model and the simulation results were compared to the measured soil moisture and isotopic composition data.

To evaluate the performance of the simulations with these parameter sets, two objective functions were applied: KGE' to compare simulated and measured soil moisture values and KGE^- to compare the simulated isotopic composition of the soil water to the measured $\delta^{18}O$ and $\delta^{2}H$ values of the soil profiles. The modified Kling-Gupta efficiency KGE' after (Gupta et al., 2009) and (Kling et al., 2012) compares simulated and observed data with regard to their correlation, their ratio of the mean values, and their ratio of the coefficient of variation. As the isotopic compositions were not measured at the study sites but at distant stations, in case of the German site at an elevation almost 1000 m lower, possible biases had to be ignored. Thus, the KGE^-, a reduced version of KGE' that only accounts for the correlation coefficient and the ratio of standard deviations, was applied to compare measured and simulated isotope data (Seeger and Weiler, 2014). The ideal value for KGE' and KGE^- is 1.

Three objective functions were used to determine the best model runs. The simulations that best fit the measured soil moisture data at the depths of the probes were identified by calculating the mean of the according KGE' values, in the following KGE'_{SM}. The mean of the KGE^- values

for the comparison of measured and simulated $\delta^{18}O$ and $\delta^{2}H$ values was calculated to determine the simulations that best represent the isotopic compositions (KGE^{-}_{Iso}). The mean of the two preceding values was used to identify the model runs that best fit to the measured soil moisture and isotope data, in the following *SM+Iso*. The Monte Carlo optimization was performed with a sample size of 750, as program limitations did not allow a higher number.

As sensitivity analysis, the parameters of the model runs with the best performances, according to the objective functions, were plotted in a cumulative distribution function. A parameter is sensitive if its distribution differs from a uniform distribution, i.e. the graph differs from the identity line.

Tab. 2: Parameter spaces for the Monte Carlo algorithm.

Parameter	Parameter space	
	Upper horizon	Lower horizon
Residual soil moisture, SM_r [cm^3 cm^{-3}]	0.130 (DE) 0.05 – 0.1 (UK)	0.076 (DE) 0.05 – 0.1 (UK)
Saturated soil moisture, SM_s [cm^3 cm^{-3}]	0.50 – 0.65 (DE) 0.35 (UK)	0.15 – 0.25 (DE) 0.32 (UK)
Inverse of the capillary fringe thickness, α [cm^{-1}]	0.001 – 0.1	0.001 – 0.1
MVG shape parameter, n [-]	1.01 – 1.85	1.01 – 1.85
Saturated hydraulic conductivity, K_s [cm day^{-1}]	0.5 – 1500	5 – 3000
Bulk density, ρ_b [g cm^{-1}]	0.6 – 2	0.6 – 2
Longitudinal dispersivity, D_l [cm]	1 – 50	1 – 50
Maximum root depth, RD_{max} [cm]	1 – 50	1 – 50

4. Results

4.1 Isotope Analysis

4.1.1 German Site

Comparing the measured and obtained stable isotope ratios to the global meteoric water line (GMWL) allows an insight into the local climatic conditions and processes. The local meteoric water line (LMWL) of the precipitation data at the German site is similar to the GMWL (Fig. 5). The soil evaporation line of all soil water samples has a slightly lower slope than the LMWL. Dividing the soil water samples into shallow and deep soil shows that the shallow soil evaporation line has the lowest slope, while the deep soil evaporation line is steeper than the LMWL. The shallow and deep soil are differently affected by local processes.

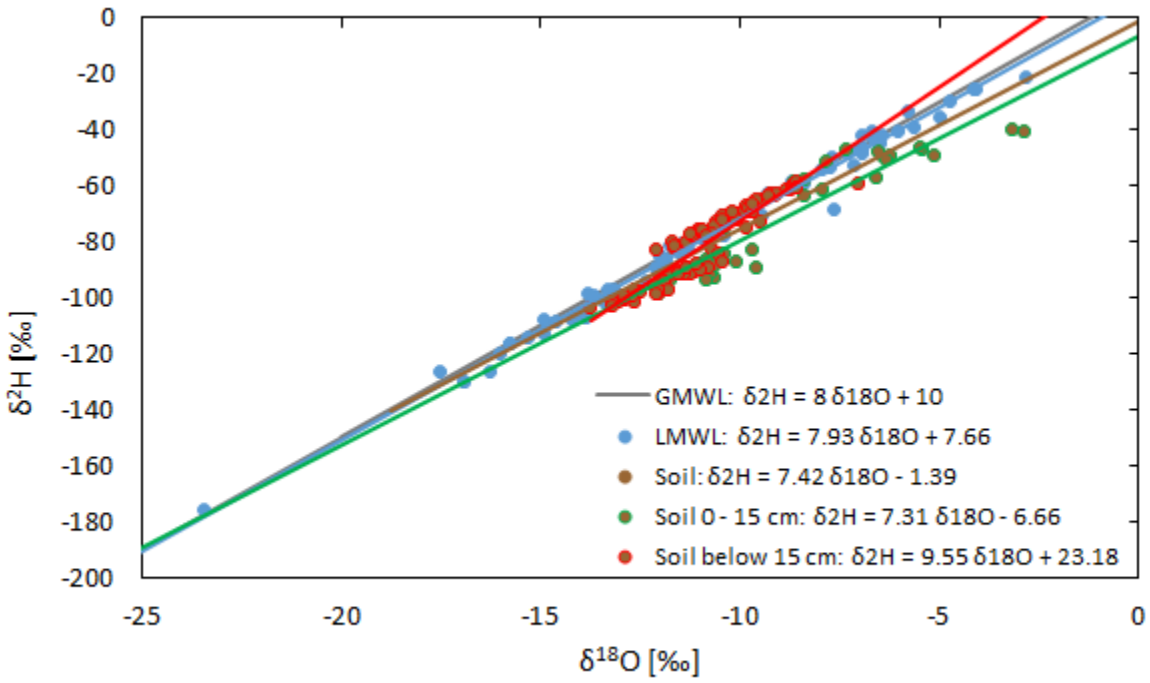

Fig. 5: Dual isotope plot at the German site. The lines represent the evaporation lines of the according soil and precipitation samples.

To investigate heterogeneity of soil properties within and between the two measurement plots, I compared the three stable isotope profiles of each plot. At the grassland, the $\delta^{18}O$ and $\delta^{2}H$ profiles have a similar shape, with the highest values at the top, decreasing until a depth of 20 cm and consistent or slightly increasing values below (Fig. 6 a, b). Profile 1 shows a peak at the 20 – 25 cm sample. The profiles at the forest plot have a similar shape compared to the grassland profiles but higher variations (Fig 6 c, d). The $\delta^{18}O$ and $\delta^{2}H$ profiles correlate well, except for a peak of $\delta^{18}O$ in profiles 1 and 2 at 10 – 15 cm that was not observed at the $\delta^{2}H$ profile. Measured $\delta^{2}H$ values of profiles 2 and 3 differ by up to 17 per mill points at 35-40 cm depth, while profile 1 has the lowest value of all profiles at 20 – 25 cm and the highest values below 40 cm. The measured isotope profiles have similar shapes but show clear variations within and between the two plots.

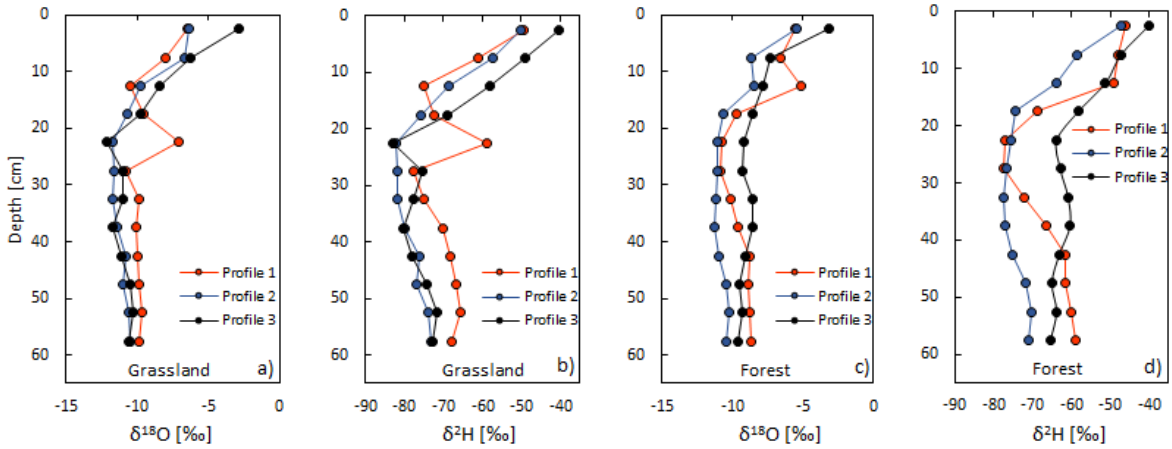

Fig. 6: Stable isotope profiles at the grassland and forest plot of the 2020 measurement campaign at the German site. Each dot represents the depth from 2.5 cm above to 2.5 cm below.

4.1.2 British Site

The dual isotope plot at the British site shows similar characteristics as at the German site (Fig. 7). The LMWL of the precipitation data is similar to the GMWL. The soil evaporation lines all have a considerably lower slope than the LMWL. Similar to the German site, the deep soil evaporation line has a steeper slope than the shallow soil. The observed $\delta^{18}O$ and $\delta^{2}H$ values are higher than the ones at the German site. The stable isotope data at the British site indicate similar processes but a stronger effect on soil water.

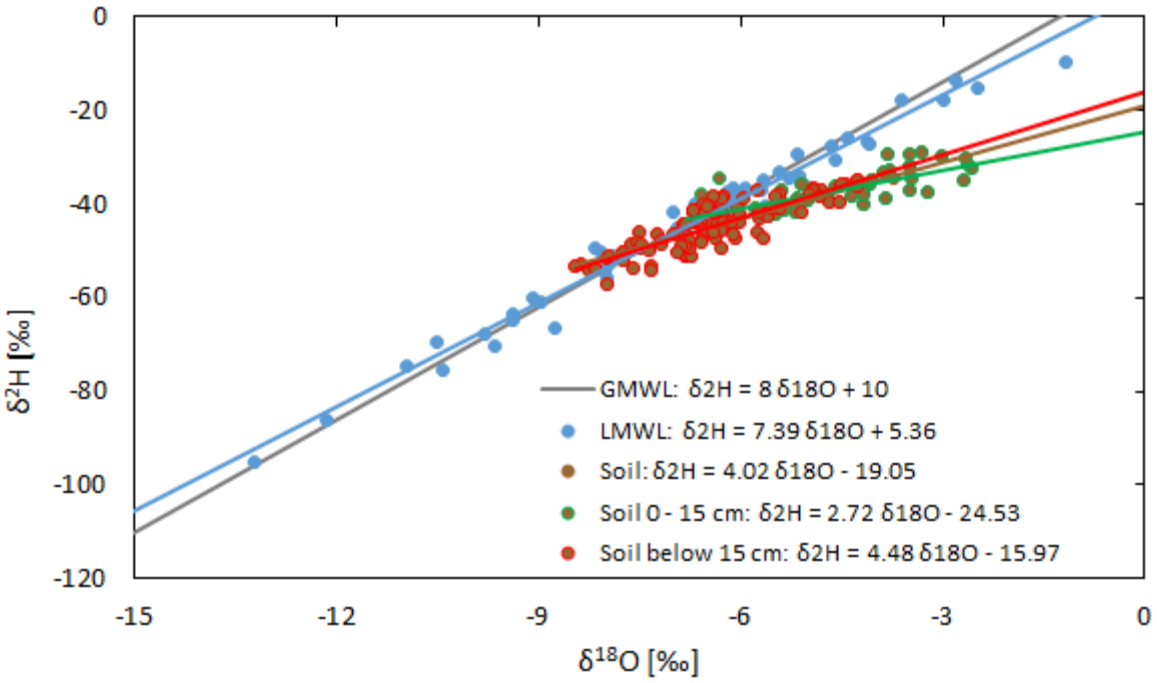

Fig. 7: Dual isotope plot at the British site. The lines represent the evaporation lines of the according soil and precipitation samples.

Heterogeneity of soil water stable isotope profiles within and between the two measurement plots was also investigated at the British site. At the grassland, the $\delta^{18}O$ and $\delta^{2}H$ profiles have a similar shape, with the highest values at the top, decreasing until a depth of 20 cm and with a weaker decrease until 50 cm (Fig. 8 a, b). The profiles at the forest plot have a different shape than the grassland profiles and higher variations (Fig. 8 c, d). Profiles 1 and 3 have a peak at 5 – 10 cm. The measurements of profile 2 differs strongly from those of the other two profiles and has a 15 per mill points lower $\delta^{2}H$ value at 55 – 60 cm depth. The $\delta^{18}O$ and $\delta^{2}H$ profiles correlate well. The three measured isotope profiles at the grassland are similar, whereas the profiles at the forest plot show strong heterogeneities in terms of shape and value range.

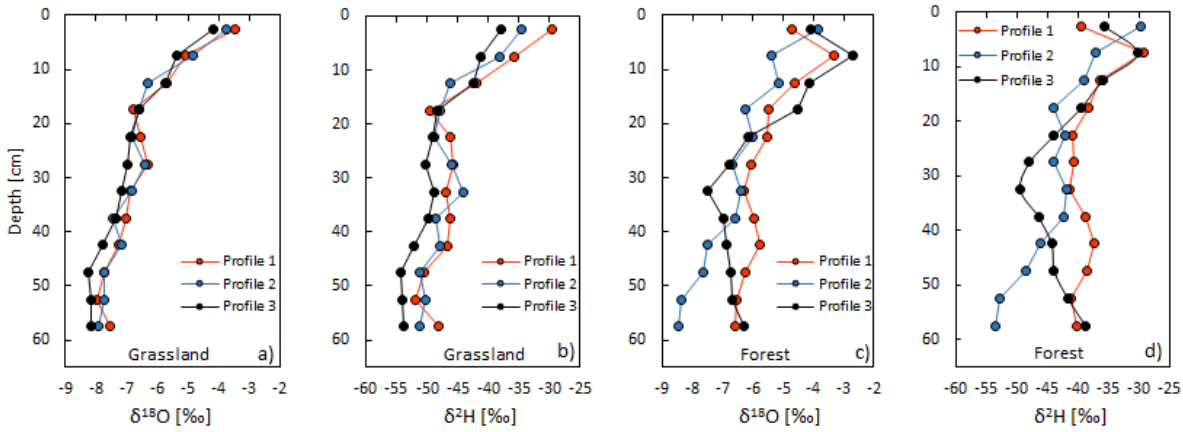

Fig. 8: Stable isotope profiles at the grassland and forest plot of the 2020 measurement campaign at the British site. Each dot represents the depth from 2.5 cm above to 2.5 cm below.

4.2 Modeling

4.2.1 German Site

The best model performances were selected by identifying the simulation runs with the highest KGE for the three objective functions. The simulation that best reproduced the measured soil moisture date, i.e. with the highest KGE'_{SM}, yielded the worst overall performance (*SM+Iso*) in this selection (Tab.3). Choosing the isotope data as optimization target (best KGE^{-}_{Iso}) produced the highest value of all KGEs and a good overall performance. The simulation with the best overall performance, i.e. highest *SM+Iso*, has similarly good KGE'_{SM} and KGE^{-}_{Iso} values and a slightly higher overall efficiency than the best KGE^{-}_{Iso} run.

Tab. 3: Goodness-of-fit measures for the best model runs according to the three objective functions at the German site. The ideal value is 1.

	KGE'_{SM}	KGE^{-}_{Iso}	*SM+Iso*
Best value for KGE'_{SM}	0.45	-0.46	-0.01
Best value for KGE^{-}_{Iso}	-0.05	0.53	0.24
Best value for *SM+Iso*	0.23	0.43	0.33

As the best simulation, I selected the model run with the highest *SM+Iso* value. The water and solute transport parameters of both model horizons for that simulation are shown in Tab. 4. The lower horizon has a considerably lower saturated soil moisture and higher saturated hydraulic conductivity value than the upper horizon.

Tab. 4: Optimized parameters for both layers at the German site.

	SM_r [-]	SM_s [-]	α [cm^{-1}]	n [-]	K_s [$cm\ d^{-1}$]	ρ_b [$g\ cm^{-3}$]	D_l [cm]
Upper horizon	0.13	0.54	0.053	1.16	1032	1.36	44.98
Lower horizon	0.08	0.19	0.048	1.69	2876	0.77	36.85

For visual evaluation of the model performance, I plotted the course over time and the values at the time of the soil water isotopic sampling of measurements and simulations for soil moisture and δ2H value, respectively. The simulation that best reproduced the measured soil moisture values has similar values for moisture in 5 and 10 cm depths throughout the model period (Fig. 9, top). During the first half of the period, these values are lower than the measured ones and the peaks do not correlate. The measured soil moistures are almost constant at a high level until June. After July, the simulations correlate well with the measured soil moisture dynamics. Simulated and measured soil moisture values at 45 cm depth are low throughout the period, the small peaks do not correlate. The simulated δ2H values, that were not regarded by this objective function, are several orders of magnitude higher than the measured ones.

The upper two soil moisture values of the simulation with the best combined performance for soil moisture and isotopic composition overestimate the measured values most of the time, most pronounced in March, May, and the beginning of August (Fig. 9, bottom). The simulated dynamics do not represent the measurements. Similar to the soil moisture optimized graph, the simulated soil moisture at 45 cm depth has equally low values as the measured ones but shows different dynamics. The simulated δ2H values have an offset of 15 ‰, compared to the measurements. The course of the simulated profile is similar, except for the peak in the middle of the profile, which starts 5 to 10 cm higher than at the measured profile. Optimizing the model parameters solely with regard to soil moisture led to good moisture simulation results at the end of the model period but yielded poor performance for δ2H values. The best model run for the objective function including soil moisture and isotopic composition performed worse for the soil moisture but produced a good fit for the δ2H profile.

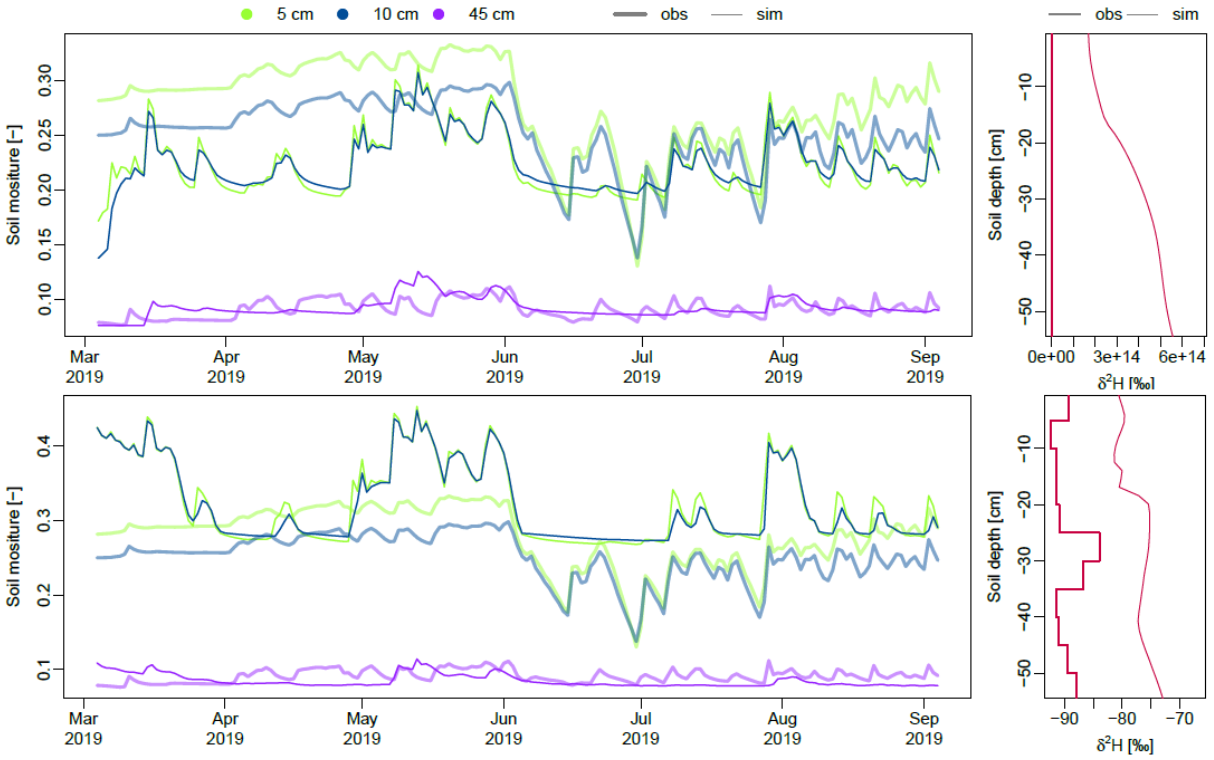

Fig. 9: Comparison of simulated and measured soil moisture values during the simulation time and of δ^2H for the simulation with the best performance for soil moisture (top) and for *SM+Iso* (bottom) at the German site.

The simulated soil moisture values throughout the soil profile indicate a distinct transition from upper to lower horizon for the overall best simulation (SM+Iso; Fig. 10). Soil moisture in the upper horizon is considerably higher than below and generally higher than the measurements. Simulated soil moistures at the lower horizon are close to 0.1 throughout the entire depth and time and similar to the measurements at 45 cm. Precipitation events lead to an increase in soil moisture, reaching lower depths at later times. Only the heaviest precipitation period in May causes a slight increase in soil moisture at the lower horizon.

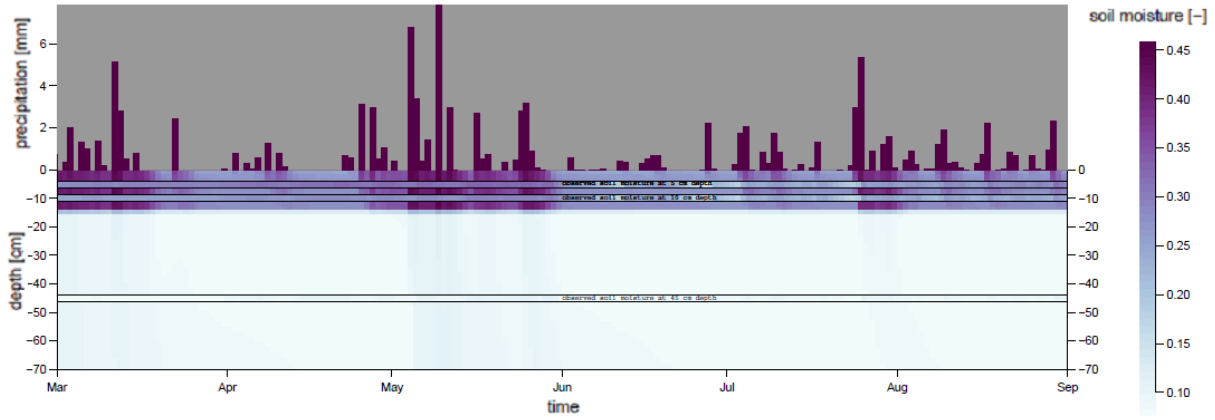

Fig. 10: Observed precipitation and simulated soil moisture across the soil profile during the simulation period, compared to measurements at 5, 10, and 45 cm depth at the German site.

The temporal course of the soil water stable isotope profiles allows an assessment of the impact precipitation has on the isotopic composition of soil water. Precipitation water contained fewer ^{2}H and ^{18}O isotopes in March to May and more in June to August, with the lowest $\delta^{2}H$ and $\delta^{18}O$ ratios in May (- 87 ‰ and - 12 ‰) and the highest in June (- 26 ‰ and - 4 ‰; Fig. 11). The $\delta^{2}H$ profile seems homogeneous at the beginning of the model period, until large amounts of lighter precipitation water in May rapidly infiltrate throughout the profile and mix with the soil water. Precipitation water in June has the highest $\delta^{2}H$ ratio but comes at low amounts and has little impact on the soil water. Larger amounts of heavier precipitation water infiltrate and change the soil water isotopic compositions until a depth of 15 cm in July and until 40 cm in August, penetrating the lower horizon. Simulated $\delta^{2}H$ ratios are higher than the values measured in June, the measured ratios are lower than the ratios of previous precipitation water. The same processes can be observed for the $\delta^{18}O$ profile (Fig. 11, bottom). Contrary to the $\delta^{2}H$ profile, the March precipitation $\delta^{18}O$ content is considerably higher than the initial soil water content and has a stronger impact on the soil water isotopic composition. Simulated $\delta^{2}H$ ratios are lower than the values measured in June.

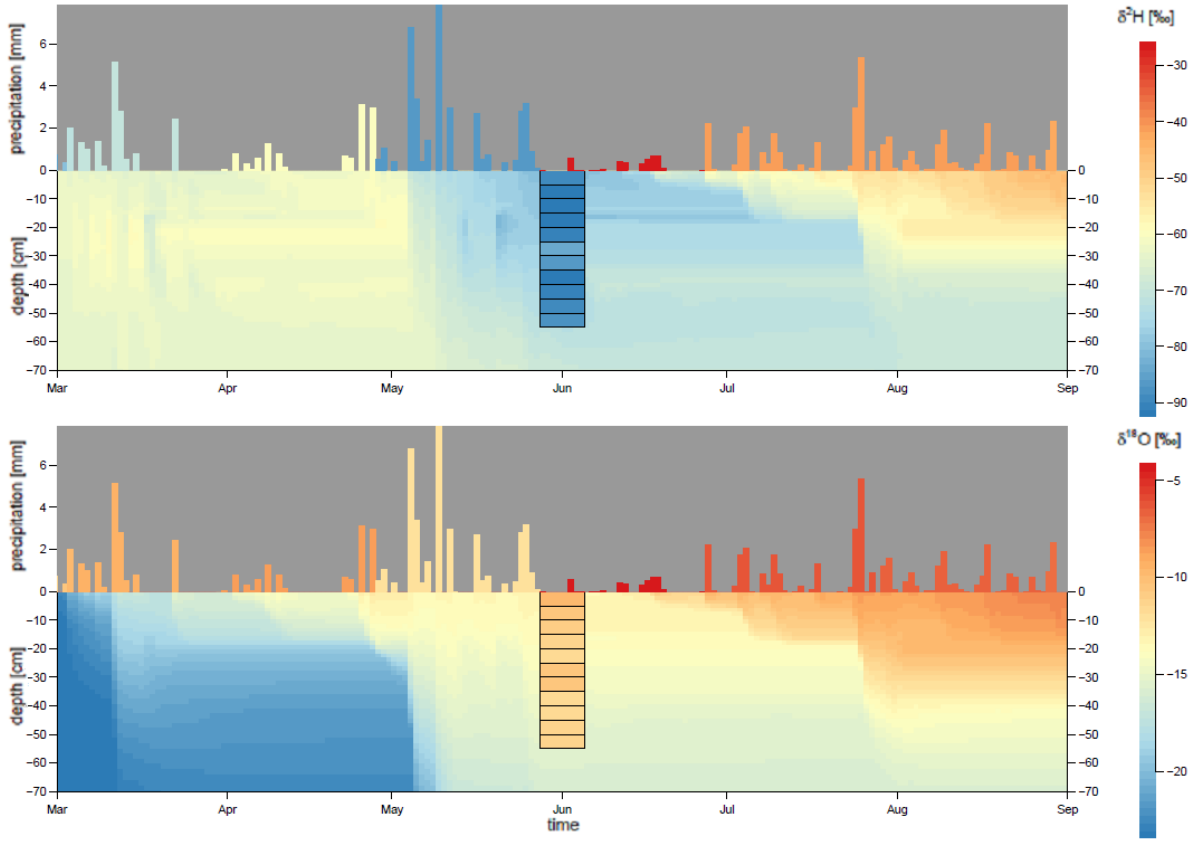

Fig. 11: Simulated δ^2H (top) and δ^{18}O (bottom) ratios across the soil profile during the simulation period compared to measurements at the German site in June 2019.

Sensitivity analysis was carried out by plotting the cumulative parameter distribution for the best model runs. The lines indicating the best 1 % of model runs deviate strongly but only represent seven measurements and were, therefore, not considered for the analysis (Fig. 12). Applying SM as objective function and regarding the best 10 %, the cumulated functions of SM_s, n, and D_l in the upper horizon have a slightly steeper slope at the beginning of the parameter range, indicating sensitivity in that area. For all objective functions, best efficiencies were achieved with K_s values above 150, other parameters showed no sensitivity for the upper horizon. For the lower horizon, SM_s is sensitive at values in the lower third of the parameter range for all objective functions. The parameter α is sensitive at values between 0.0 and 0.02 for SM and SM+Iso, and for values below 0.05 for Iso. The shape parameter n and the saturated hydraulic conductivity are sensitive at the upper part of the parameter range for all objective functions. The longitudinal dispersivity is sensitive for Iso and SM+Iso. Cumulated parameter distributions of the best model runs indicate sensitivity for three parameters in the upper horizon, two of them only for the objective function SM. In the lower horizon, five of the six parameters showed sensitivity, differently pronounced for the three objective functions.

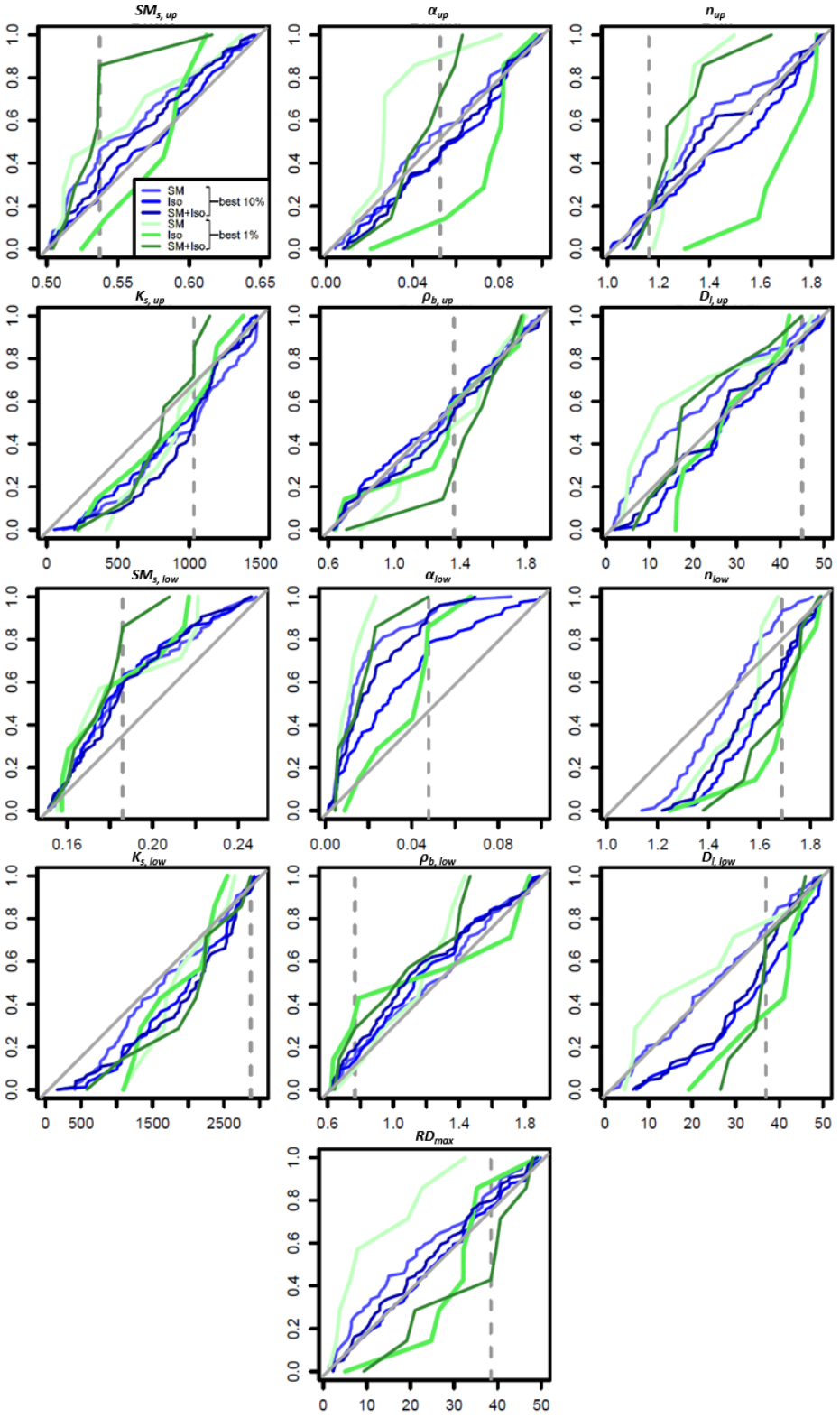

Fig. 12: Cumulated parameter distributions for the best model runs for the German site; divided into upper (rows 1 and 2) and lower horizon (rows 3 and 4). The dashed lines indicate the values for the best simulation.

4.2.2 British Site

Equally to the German site, the best model performances were selected by identifying the simulation runs with the highest KGE for the three objective functions. The simulation best reproducing the measured soil moisture data (highest KGE'_{SM}) achieved the highest KGE value but a highly negative KGE^{-}_{Iso} and the worst overall performance in this selection (Tab.5). The simulation run with the highest KGE^{-}_{Iso} also produced the best overall performance. The relatively low KGE^{-}_{Iso} is the mean of a high efficiency for δ^2H values and a low efficiency for δ^{18}O values. The simulations for the British site better reproduced the measured soil moistures but performed worse for KGE^{-}_{Iso} and *SM+Iso*, compared to the German site.

Tab. 5: Goodness-of-fit measures for the best model runs according to the three objective functions at the at the British site. The ideal value is 1.

	KGE'_{SM}	KGE^{-}_{Iso}	*SM+Iso*
Best value for KGE'_{SM}	0.57	-1.66	-0.55
Best value for KGE^{-}_{Iso}	0.09	0.19[a]	0.14
Best value for *SM+Iso*	0.09	0.19[a]	0.14

[a] KGE^{-}_{2H}: 0.70; KGE^{-}_{18O}: -0.32

Analogous to the German site, I selected the model run with the highest *SM+Iso* value as the best simulation. The water and solute transport parameters of both model horizons for that simulation are shown in Tab. 6. Residual and saturated soil moisture are similar for both horizons. The lower horizon has considerably higher values for α, saturated hydraulic conductivity, and longitudinal dispersivity.

Tab. 6: Optimized parameters for both layers at the British site.

	SM_r [-]	SM_s [-]	α [cm^{-1}]	n [-]	K_s [cm d^{-1}]	ρ_b [g cm^{-3}]	D_l [cm]
Upper horizon	0.07	0.35	0.008	1.52	438	0.93	14.46
Lower horizon	0.07	0.32	0.074	1.04	2316	1.18	40.47

Comparison of simulated and measured soil moisture and δ2H values provides additional information on the model performances. The simulation that best reproduces the measured soil moisture values has almost identical values for moisture in 5 and 10 cm depths throughout the model period (Fig. 13, top). These simulated values have a similar course compared to the measurements for most of the model period but underestimate the measured peaks. At 39 cm depth, the simulation produced considerably lower values than the measurements. The simulated soil moisture decreases almost constantly after March; the measured soil moisture has a similar value range as at 5 and 10 cm and has one high peak in June. The simulated δ2H profile, which was not regarded by this objective function, is almost a constant line at the mean of the measured values. The low and high δ2H values that were measured at 10 – 15 cm and 45 – 50 cm depths, respectively, are not reproduced by the simulation.

The upper two soil moisture series of the simulation with the best combined performance for soil moisture and isotopic composition strongly underestimate the measured soil moisture throughout the period (Fig. 13, bottom). The simulated peaks are at similar times as the measured ones but at a lower magnitude. Simulated soil moisture at 45 cm depth is almost constant at 0.26 throughout the period, not showing the measured temporal variations. The simulated δ^2H values are consistently lower than the measurements and the course of the simulated profile is similar, except for the maximum of δ^2H, which was measured at 10 – 15 cm and simulated at 20 cm depth. Optimizing the model parameters solely with regard to soil moisture led to a good reproduction of the measured soil moisture dynamics at the top of the profile but yielded a poor performance for the soil moisture at the bottom and for the δ^2H profile. The best model run for the objective function including soil moisture and isotopic composition performed worse for the soil moisture but produced a good fit for the δ2H profile.

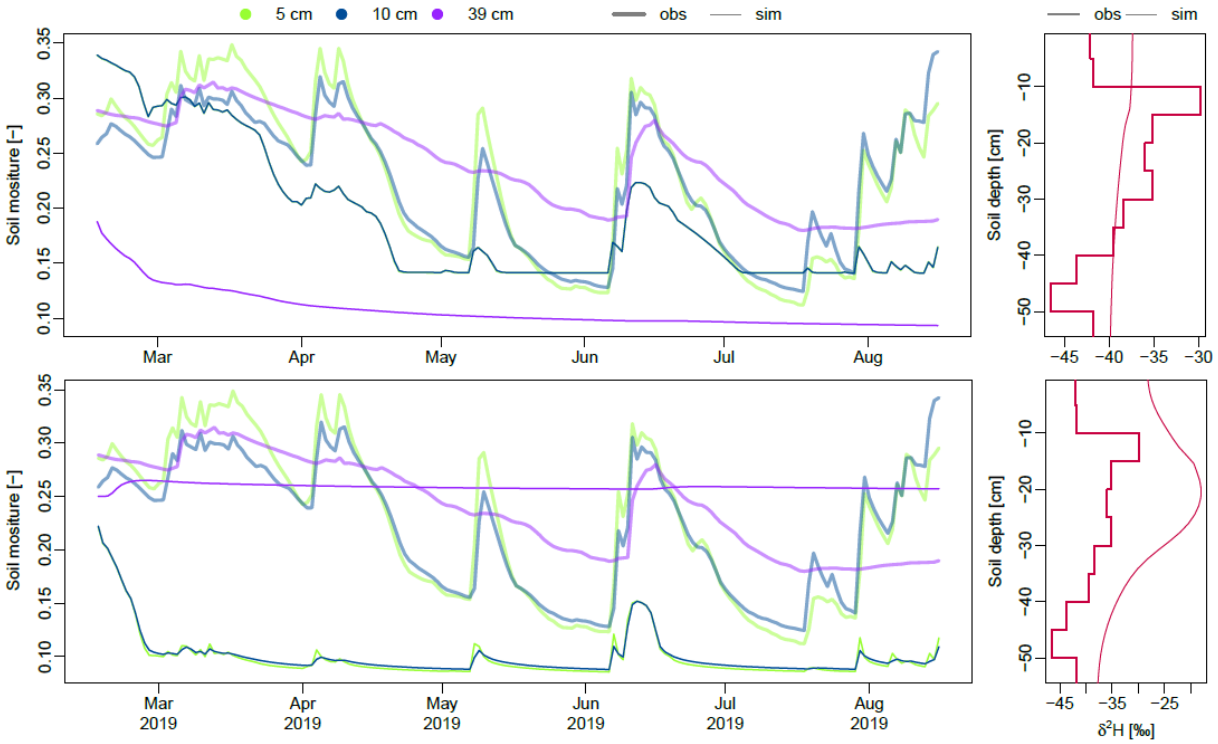

Fig. 13: Comparison of simulated and measured soil moisture values during the simulation time and of δ^2H values for the simulation with the best performance for soil moisture (top) and for *SM+Iso* (bottom) at the British site.

The simulated soil moisture values throughout the soil profile indicate a distinct transition from upper to lower horizon for the overall best simulation (SM+Iso; Fig. 14). The characteristics are opposite to those at the German site. Soil moisture in the upper horizon is close to 0.1 throughout the profile and period and generally lower than the measurements. Simulated soil moistures at the lower horizon are considerably higher than above and do not deviate strongly throughout the period, contrary to the measurements. There is less precipitation than at the German site. Rain events led to a slight increase in soil moisture in the upper horizon, only the heaviest events at the end of May had an impact on the lower horizon.

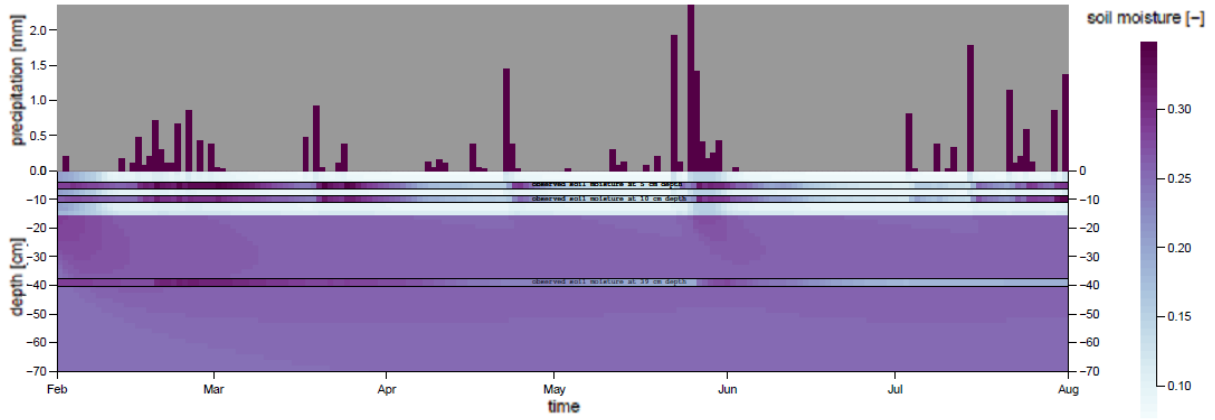

Fig. 14: Observed precipitation and simulated soil moisture across the soil profile during the simulation period, compared to measurements at 5, 10, and 39 cm depth at the British site.

The impact of precipitation water on the soil water stable isotope composition can be observed from the temporal course of isotopic profiles. Isotopic compositions of precipitation water deviate slightly, with the lowest $\delta^{2}H$ and $\delta^{18}O$ ratios in July (Fig. 15). The low precipitation amounts in the first half of the model period only infiltrate and change the isotopic composition in the upper 10 to 15 cm. Higher precipitation amounts at the end of May impact the isotope profiles until a depth of 20 to 30 cm. Below 30 cm, the profiles are not affected by precipitation water throughout the model period and dominated by the initial conditions. This can be observed for both, $\delta^{2}H$ and $\delta^{18}O$, profiles.

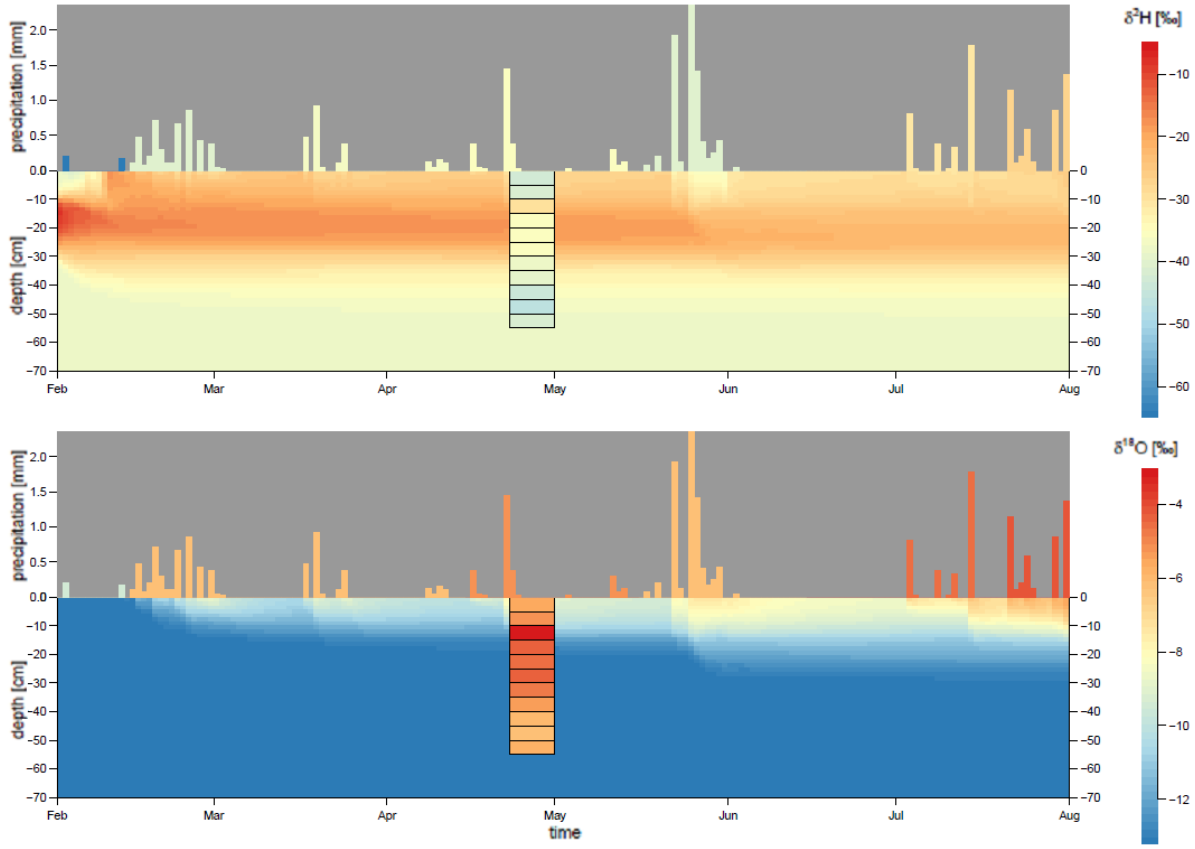

Fig. 15: Simulated δ^2H (top) and δ^{18}O (bottom) ratios across the soil profile during the simulation period compared to measurements at the British site in June 2019.

The optimized parameters were investigated for sensitivity in the same way as for the German site. The distributions at the upper horizon show weak sensitivity for SM_r, K_s, ρ_b, and D_l (Fig. 16). For α, the cumulated functions of the best 1 % indicate a high sensitivity for all objective functions at values below 0.02. The functions of the best 10 % show sensitivity for SM only. The parameter n is sensitive for SM at values between 1.1 and 1.4 and highly sensitive for Iso and SM+Iso at values close to 1.0. In the lower horizon, n is the only sensitive parameter. It is sensitive for Iso and SM+Iso at values close to 1.0 and above 1.6, and for SM at values between 1.1 and 1.6. The maximum rooting depth is not sensitive. Cumulated parameter distributions of the best model runs indicate sensitivity for two parameters in the upper horizon, one of them only for the objective function SM. In the lower horizon, only one parameter is sensitive but at different values for SM than for the other objective functions.

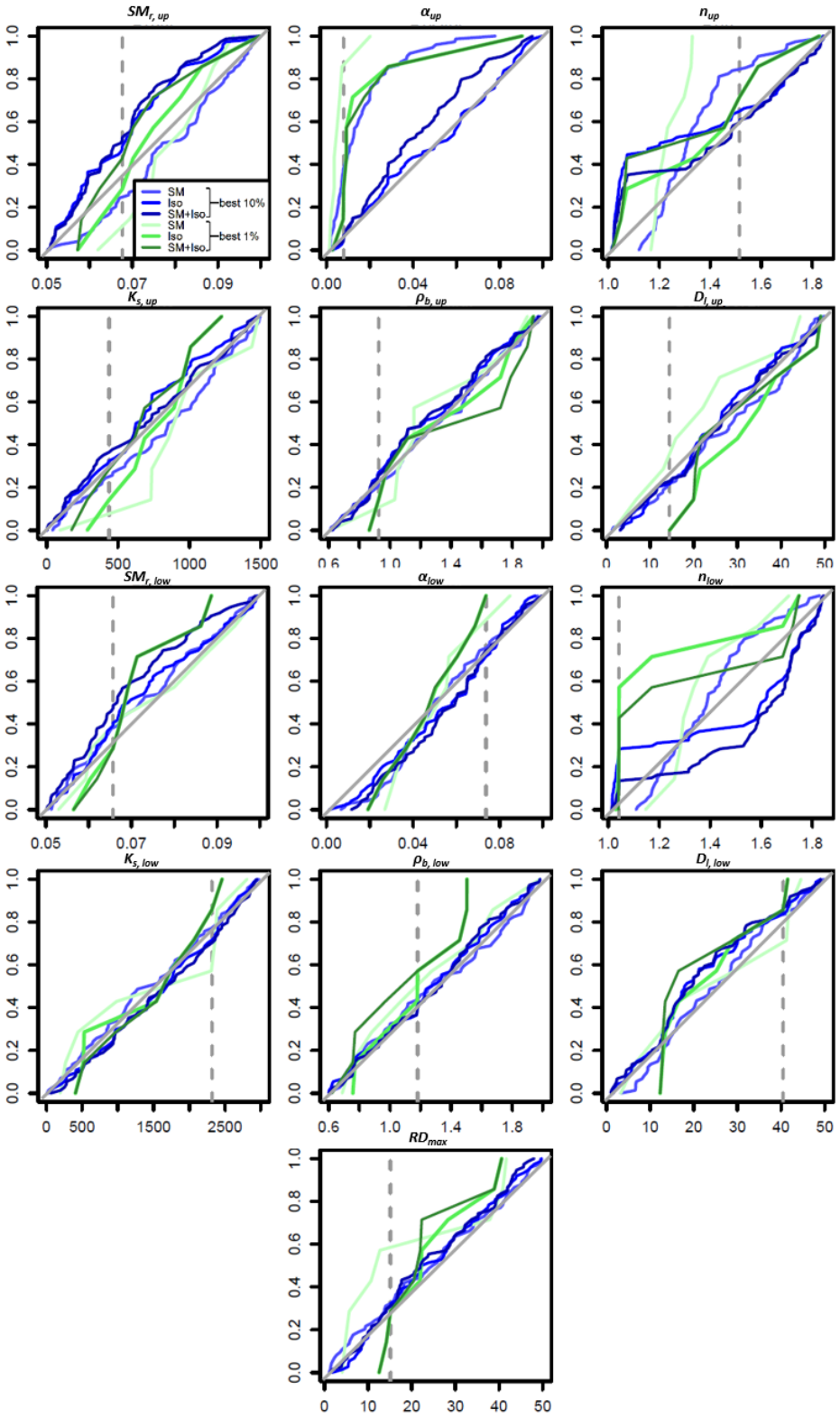

Fig. 16: Cumulated parameter distributions for the best model runs for the British site; divided into upper (rows 1 and 2) and lower horizon (rows 3 and 4). The dashed lines indicate the values for the best simulation.

5. Discussion

5.1 Model Evaluation

The soil hydraulic model used to simulate water flow and isotope transport in the vadose zone and the input parameters have several limitations and shortcomings. The soil moisture sensors used in the field are not calibrated and, therefore, only detect the course of soil moisture but not the actual water content which is required by the program. This may cause inaccuracies. Another inaccurate input parameter is the precipitation water isotopic composition, as the samples were not taken at the study sites. This is more pronounced for the German site, where samples were taken at a far lower elevation and at the opposite site of a mountain range. The model accounts for this by ignoring a bias for the calculation of efficiencies. This may not be sufficient, as precipitation water undergoes various fractionation processes before reaching the study site or the weather station. This possibly causes a non-uniform deviation of the isotopic concentrations. Moreover, the isotopic composition of precipitation water is determined from a composite sample of all precipitation water in one month, not accounting for variability during that period.

The hydraulic model is limited to two horizons and the Richards equation assumes homogeneous soil properties throughout each layer. Hence, it does not account for heterogeneities or a third horizon as observed at the German site. The selected snow model is a simple approach to account for precipitation water accumulating on top of the soil profile instead of infiltrating. It assumes a mixing of the snow resulting in a homogeneous isotopic composition of the meltwater and does not account for natural processes like sublimation enrichment of heavy isotopes (Ala-Aho et al., 2017).

Since the efficiency of the pore water isotope simulations is highly dependent on the isotopic signal of the rainwater, a sufficiently long input time series is crucial in order to ensure that the initial pore water has been replaced. Thus, adding a warm-up period could improve model performance and realism. It would also allow a snow cover to accumulate over the winter at the German site. The period should preferably exceed the mean transit time of water in the soil profile. Including a warm-up period of one year did, however, not improve or even worsen the model performance. This was due to a program error causing highly unrealistic stable water isotopic concentrations at the beginning of the periods. The source of this error could not be identified during this study.

Another so far undetected error does not allow the program to continue its calculations after 750 to 800 model runs. This limits the sample size of the Monte Carlo sampling to 750, which is insufficient to produce satisfactory results or perform a conclusive sensitivity analysis. Other studies with an inverse soil hydraulic model used a sample size of 5000 per input parameter (Zhou et al., 2012). This would enable a more detailed sensitivity by dividing simulation results into good and best model runs.

Despite these limitations and shortcomings, the soil hydraulic model was able to produce simulations with good efficiency values and several sensitive parameters. It also confirmed a positive impact of including pore water stable isotopes into the calibration process on model realism.

5.2 Isotope Analysis

The local meteoric water lines at both locations are similar to the GMWL, indicating average humid climatic conditions. The soil evaporation lines have, with one exception, a lower slope than the lines obtained from precipitation water. This is caused by fractionation processes due to evaporation and especially affects the upper soil. The soil evaporation lines at the British site deviate stronger from the LMWL, indicating a stronger influence of evaporation caused by a more arid climate, compared to the German site. This is in accordance with a lower average temperature and a double amount of precipitation at the German site. The soil evaporation line of the lower soil at the German site being steeper than the LMWL might indicate that the LMWL at the weather station is not equal to the one directly at the study site. Precipitation and soil water at the British site generally contain more heavy stable water isotopes than at the German site. This is an effect of shorter distance to the sea, lower altitude, and higher average temperature, each allowing fewer fractionation processes compared to the German site. The observed stable water isotope concentrations show typical characteristics of the local climatic conditions.

Varying environmental conditions and soil properties can cause variations of isotopic profiles at a local scale (Clark and Fritz, 1997). The depth profiles of $\delta^{18}O$ and $\delta^{2}H$ at the two plots of the study sites give an impression of local vegetation- and soil-related heterogeneities. Almost all profiles show an evaporation front directly below the surface. The higher concentrations of ^{18}O and ^{2}H are caused by evaporation-induced fractionation, leaving a higher fraction of heavy isotopes in the soil. The three grassland profiles at the German site indicate relatively homogeneous conditions throughout the plot. The forest profiles show stronger deviations. This

can be caused by heterogeneities of soil structure or by the more diverse vegetation, affecting root distribution and interception of rainwater. Both were observed in the field. Similar observations can be made at the British site, also indicating stronger heterogeneities within the forest plot. At two profiles from the forest, the evaporation front is shifted to a lower depth. This is caused by recently infiltrated rainwater that had not been exposed to evaporation as much as older soil water. At both sites, isotopic profiles indicate homogeneous soil properties within the grassland plots and higher deviations within the forest plots, most likely caused by heterogeneous vegetation and soil structure.

5.3 Simulation Results

5.3.1 German Site

The goodness-of-fit measures for the best simulations for the German site show strong variabilities, depending on the objective function. For KGE, the efficiency value of using the mean value as predictor is -0.41 (Knoben et al., 2019). Thus, KGE values higher than -0.41 indicate an improvement upon the mean value benchmark. The model run best reproducing the measured soil moisture achieved moderately high efficiency for KGE'_{SM} but fails to account for the measured isotopic compositions. The according efficiency value KGE^{-}_{Iso} is below -0.41. Thus, the model failed to produce realistic transport parameters and does not depict the natural processes. Similar observations are made for the simulation best reproducing the measured isotopic compositions. It produces a high efficiency for the isotope data but has a rather weak performance for soil moisture. The strongly different efficiency values of these two simulations indicate that they describe different transport processes within the soil. The best overall simulation produced acceptable to good efficiencies for both parameters. These results show an advantage of including soil moisture isotope data into soil hydraulic modeling. Using only either one of the parameters would give the impression of a good model performance despite not depicting the real transport processes.

The optimized parameters indicate different soil types for the two horizons. The higher saturated soil moisture, thus higher water storage capacity, and the lower saturated conductivity of the upper horizon are characteristics of a finer textured soil. This corresponds to observations made in the field. The saturated hydraulic conductivities in both horizons exceed those of a typical sandy soil (Carsel and Parrish, 1988). This does not match the field observations of a

silty clay texture but might be realistic due to preferential flow along rocks or channels in the soil matrix.

Simulated soil moisture values in the upper horizon deviate strongly from the measured values in the first half of the model period. For both simulations, optimized for soil moisture only and the combination of soil moisture and isotopic composition, soil moisture curves react to precipitation events in March and May. The measured values remain almost constant at a high level during that time. This indicates that precipitation fell as snow and did not infiltrate immediately. This is not depicted by the included snow model of the program. The model performances at the beginning of the period are also affected by the lack of a warm-up period. While snow accumulated over the entire winter in the field, the model starts its calculations without a snow cover in March. The clear transition of simulated soil moistures between the two horizons is caused by the low saturated soil moisture and high hydraulic conductivity in the lower horizon. These do not allow the soil to store large amounts of water and induce a fast transport through the lower model boundary. In accordance to the goodness-of-fit measures, including isotopic data into the parameter optimization reduces the accuracy of modeled soil moisture but still allows a good representation of measured values.

Stable water isotope concentrations in precipitation water are subject to seasonal variations. Rainwater generally contains more heavy ^{18}O and ^{2}H isotopes at high temperatures in summer. This can also be observed for precipitation data obtained from the weather station near the study site. It is, however, unusual that the lowest and the highest concentrations were observed in two successive months. This can be explained by the precipitation amount. Heavy rainfall events like the ones in May usually contain fewer heavy isotopes, while small events like in June are enriched. Correspondingly to the goodness-of-fit measures, comparison of simulated and measured isotopic data shows a good accordance. The bias is most likely caused by the distant location of precipitation sampling. As isotopic composition of precipitation water is only measured once a month from a composite sample, some precipitation events during that month might contain higher or lower stable isotope concentrations. This explains the measured samples having lower $\delta^{2}H$ values than observed in previous precipitation. Two factors benefit good simulation results for the isotope profiles. There had been enough precipitation in the previous months, allowing water of a known isotopic composition to infiltrate through the entire profile. In addition, that precipitation water had varying isotopic signatures, allowing to distinguish the temporal origin of soil water.

Four sensitive parameters could be identified for the upper horizon using SM as objective function. None of them, however, showed a strong sensitivity and good results were achieved with parameter values across a wide range. Including or only using stable isotope data in the objective function reduced the number of sensitive parameters to one. Hence, it reduced the parameter identifiability. Hydraulic conductivity is a decisive transport parameter and sensitive for all objective functions. Sensitivity analysis for the lower horizon produced more and stronger sensitivities. The transport parameter D_l is not sensitive for soil moisture. All other parameters, except bulk density, show sensitivity for each objective function. Including isotope data in the model slightly increased parameter identifiability in the lower horizon. Modeling the transport of stable water isotopes also allows to determine the longitudinal dispersivity. As this transport parameter showed sensitivity in both layers, it is an important characteristic for the soil hydraulic model and increases model realism. This is in accordance to the findings of (Sprenger et al., 2015b). Including stable isotope data into the soil hydraulic model decreased parameter identifiability in the upper horizon and slightly increased it in the lower horizon. The quality of the sensitivity analysis is, however, limited by the small sample size.

The soil hydraulic model was able to satisfactory reproduce the observed soil moisture and stable isotope measurements at the German site. Including isotopic data into the model reduced the performance of simulated soil moisture but increased model realism and allowed the determination of longitudinal dispersivity. Using only soil moisture for parameter optimization gives a false image of a good model. It produces accurate soil moisture values but fails to realistically depict transport of stable water isotopes; hence, the actual movement of water in the soil matrix. Including isotope transport into the model decreased identifiability for some and increased it for other parameters. A larger sample size for the Monte Carlo Sampling would improve parameter identification and probably also model performance.

5.3.2 British Site

The goodness-of-fit measures for the best simulations for the British site also show strong variabilities, depending on the objective function. The model run best reproducing the measured soil moisture achieved a relatively high efficiency for KGE'_{SM} but like at the German site fails to account for the measured isotopic compositions. This model therefore failed to produce realistic transport parameters and does not depict the natural processes. The simulation best reproducing the measured isotopic compositions achieved relatively low efficiencies, however,

the KGE^{-}_{Iso} value must be considered in a differentiated way. The model has a high efficiency for the ^{2}H profile. The relatively low goodness-of-fit measure for the isotope profile is caused by a bad reproduction of ^{18}O data. As ^{2}H and ^{18}O are highly correlated, this discrepancy is most likely caused by the initial conditions in the soil matrix. The simulation best reproducing the measured isotopic composition also has the highest overall model efficiency. This suggests that the best approximation of the soil hydraulic properties can be obtained by using only the isotopic data of a single soil core and the precipitation input. This was also observed for sandy soils by Mattei et al. (2020). However, the overall low efficiency values indicate that the model could not accurately reproduce the measured soil moisture values and stable isotope concentrations.

The optimized parameters show similar values for residual and saturated soil moisture for the two horizons. The upper horizon has a low α value, i.e. a thick capillary fringe. The saturated hydraulic conductivity is similar to that of a loamy sand (Carsel and Parrish, 1988), contrary to the observations in the field. The lower horizon has a saturated hydraulic conductivity three times higher than that of a sandy soil (Carsel and Parrish, 1988). This, too, is inconsistent with the observations made in the field.

The model optimized for only soil moisture produces similar results to the measurements in the upper horizon throughout the period but does not reproduce the dynamics of the lower measurements. As the simulations almost constantly underestimates the measurements, this indicates that too much water leaves the profile of the model. This is most likely due to an overestimated hydraulic conductivity. The according simulated isotope profile shows no variation and is a poor fit for the measurements. As mentioned above, this indicates a failure to depict the actual transport processes in the field. The model optimized for soil moisture and isotope concentration strongly underestimates soil moisture in the upper horizon and does not account for variations of the lower measurements. Therefore, it also fails to reproduce the natural processes, despite a good estimation of the ^{2}H profile. The constant simulated soil moistures at 39 cm depth indicate, that precipitation water does not reach this depth at both models. This is contrary to the measured responses after rain events in the field. The soil hydraulic model could not satisfactorily reproduce the observations made in the field.

Precipitation at the British site comes at lower amounts and with smaller variations of isotopic composition. Both factors make calibration of the soil hydraulic model more difficult, as it relies on precipitation water as input signal. The smaller variations of isotopic signature are due to a shorter distance to the sea and smaller temperature variations compared to the German site.

The low precipitation amounts at the beginning of the model period are a major problem for model calibration. The simulated isotope profiles show that the isotopic composition of the soil water is dominated by the initial conditions. It is not replaced by new precipitation water at most depths. The good and poor fits of the simulated ^{2}H and ^{18}O profiles, respectively, are therefore not the result of a good or poor model performance but rather of the initial concentrations in the simulated profiles. This problem could be solved by including a warm-up period. A trial simulation including a warm-up period of one year, however, did not improve the model performance. The simulated isotope profile of that simulation indicated that precipitation water only infiltrated until a depth of 30 cm. This shows that the model assumes a long transit time of water through the soil matrix. To fully replace the initial water, a warm-up period of several years would be needed. This assumption, however, is contrary to the observed quick response of soil moisture at 39 cm depth to precipitation events.

Only few sensitive parameters could be identified at the British site. In both horizons, the shape parameter *n* is sensitive for each objective function but at different values for SM than for the objective functions including stable isotope data. The parameter α in the upper layer is sensitive only for the SM objective function. Thus, including stable isotope data into the soil hydraulic model decreased parameter identifiability. The low overall parameter identifiability is in accordance with the bad model performance, as the identified parameters could not satisfactorily describe the hydraulic processes in the field. Thus, this sensitivity analysis did not produce conclusive results.

The soil hydraulic model was not able to satisfactory reproduce the observed soil moisture and stable isotope measurements at the British site. It was able to depict the measured soil moisture data but failed to do so for the stable isotope concentrations. Similarly to the German site, using only soil moisture for parameter optimization gives a false image of a good model. Simulations showed that a warm-up period of several years has to be included for sites with a long transit time of precipitation water through the soil matrix. This is necessary to replace soil water with unknown isotopic composition.

5.4 Evaluation of the Model Approach

This study supports the findings by others stating that the more data types are used for the calibration process, the lower is the model's performance with respect to different specific objective functions. Including stream water chloride (Kuczera and Mroczkowski, 1998) or isotope concentrations (Fenicia et al., 2008; Hartmann et al., 2012) in the optimization process

of a catchment model has shown to reduce stream discharge simulation efficiency but increased model realism and parameter identifiability. This effect was also shown for the use of isotope concentrations on the field scale (Sprenger et al., 2015b; Mattei et al., 2020). The present study is in line with these findings and showed this approach to be effective in karstic areas. Including isotopic information increased model realism for the German site. It did not increase parameter identifiability. However, the conclusiveness of the sensitivity analysis was strongly limited by a small Monte Carlo sample size. For the British site, the inclusion of isotopic information did not yield a realistic model but proved the model with high efficiencies concerning only soil moisture to be unrealistic.

This model approach depends on temporal variations of the precipitation isotopic composition and on precipitation water of known isotope signature thoroughly infiltrating through the observed soil profiles. It is also limited to environments where soil evaporation plays a minor role as it does not account for fractionation processes. This might be problematic in arid regions or sites with small infiltration rates. The performance and realism of the model approach can be enhanced by modeling longer time series and performing several stable isotope measurements, preferably at different seasons and hydrological states.

Considering isotope data in soil hydraulic models creates the possibility to trace water movement through the soil. It allows to determine the dispersion of the water during the percolation processes and provides the opportunity to apply particle tracking of the precipitation water, which would not be possible with a model approach limited to hydrometric data. This can be used to predict not only response time but also transit time of soil water and provides additional valuable information for a better understanding of the hydrological processes in the soil.

Including isotope data into soil hydraulic modeling generally improves model realism. An increased parameter identifiability, as shown in previous studies, could not be obtained in this study. The present approach can be used at a wide range of model sites with possible limitations in arid areas and areas with low variances of precipitation isotope signature. It allows particle tracking and thereby a more detailed insight into soil hydraulic processes.

6. Conclusion

The main goal of this study was to investigate the applicability of a soil hydraulic model to identify soil hydraulic parameters in the shallow karst vadose zone. Continuous soil moisture measurements and stable water isotope concentrations in a soil core were used to calibrate the model. This was done for two study sites, one with a humid continental climate in the Bavarian Limestone Alps and one with a temperate oceanic climate in southern England. The model satisfactorily described the transport and storage processes at the German site despite several simplifications and software limitations. Including isotope data into the inverse model did not increase parameter identifiability as the sensitivity analysis was limited by a small Monte Carlo sample size. It also led to reduced model efficiencies. However, this comes at the benefit of improved model realism. By accounting for both, soil moisture dynamics and water transport through the soil matrix, this approach allows to identify unrealistic models that only achieve high efficiencies for soil moisture simulations but fail to describe isotope transport. Furthermore, it enables particle tracking through the soil matrix, giving a detailed insight into transport and storage processes.

The model failed to describe the soil hydraulic processes at the British site. Locations with low precipitation amounts and low infiltration rates require long warm-up periods that allow precipitation water of known isotopic signature to thoroughly infiltrate into the soil profile. Whether a modeling period of several years can improve the model performance is to be investigated in future studies. A larger Monte Carlo sample size would improve both, the model performance, and the parameter identifiability.

Water flow and storage processes in the shallow karst vadose zone can be described by a soil hydraulic model. Including soil water stable isotope data improves model realism and allows further insights into soil hydraulic processes with little extra effort.

7. References

Ala-Aho, P., Tetzlaff, D., McNamara, J.P., Laudon, H., Kormos, P., Soulsby, C., 2017. Modeling the isotopic evolution of snowpack and snowmelt: Testing a spatially distributed parsimonious approach. Water Resour. Res. 53 (7), 5813–5830.

Aley, T.J., Kirkland, S.L., 2012. Down but not straight down: significance of lateral flow in the vadose zone of karst terrains. Carbonates Evaporites 27 (2), 193–198.

Aquilina, L., Ladouche, B., Dörfliger, N., 2006. Water storage and transfer in the epikarst of karstic systems during high flow periods. Journal of Hydrology 327 (3-4), 472–485. https://www.sciencedirect.com/science/article/pii/S0022169405006475.

Bakalowicz, M., 2003. The Epikarst, the Skin of Karst. Karst Waters Institute Special Publication 9, 16–22.

Benavente, J., Vadillo, I., Carrasco, F., Soler, A., Liñán, C., Moral, F., 2010. Air Carbon Dioxide Contents in the Vadose Zone of a Mediterranean Karst. Vadose Zone Journal 9 (1), 126.

Berthelin, R., Hartmann, A., 2020. The Shallow Subsurface of Karst Systems: Review and Directions. In: P. Renard (Editor), Eurokarst 2018, Besançon. Advances in the Hydrogeology of Karst and Carbonate Reservoirs. Springer International Publishing, Cham, pp. 61–68.

Berthelin, R., Rinderer, M., Andreo, B., Baker, A., Kilian, D., Leonhardt, G., Lotz, A., Lichtenwoehrer, K., Mudarra, M., Padilla, I.Y., Pantoja Agreda, F., Rosolem, R., Vale, A., Hartmann, A., 2020. A soil moisture monitoring network to characterize karstic recharge and evapotranspiration at five representative sites across the globe. Geosci. Instrum. Method. Data Syst. 9 (1), 11–23. https://gi.copernicus.org/articles/9/11/2020/.

Birkel, C., Tetzlaff, D., Dunn, S.M., Soulsby, C., 2011. Using lumped conceptual rainfall–runoff models to simulate daily isotope variability with fractionation in a nested mesoscale catchment. Adv.Water Resour. 34 (3), 383–394. https://abdn.pure.elsevier.com/en/publications/using-lumped-conceptual-rainfall-runoff-models-to-simulate-daily-.

Brinkmann, N., Seeger, S., Weiler, M., Buchmann, N., Eugster, W., Kahmen, A., 2018. Employing stable isotopes to determine the residence times of soil water and the temporal origin of water taken up by Fagus sylvatica and Picea abies in a temperate forest. New Phytologist 2018 (219), 1300–1313.

Byrne, K.A., Kiely, G., Leahy, P., 2005. CO2 fluxes in adjacent new and permanent temperate grasslands. Agricultural and Forest Meteorology 135 (1-4), 82–92.

Carsel, R.F., Parrish, R.S., 1988. Developing joint probability distributions of soil water retention characteristics. Water Resour. Res. 24 (5), 755–769.

Charlier, J.-B., Bertrand, C., Mudry, J., 2012. Conceptual hydrogeological model of flow and transport of dissolved organic carbon in a small Jura karst system. Journal of Hydrology 460-461, 52–64.

Chen, Z., Goldscheider, N., Auler, A.S., Bakalowicz, M., Broda, S., Drew, D., Hartmann, J., Jiang, G., Moosdorf, N., Richts, A., Stevanovic, Z., Veni, G., Dumont, A., Aureli, A., Clos, P., Krombholz, M., 2017. World Karst Aquifer Map (WHYMAP WOKAM).

Christiansen, J.R., Elberling, B., Jansson, P.-E., 2006. Modelling water balance and nitrate leaching in temperate Norway spruce and beech forests located on the same soil type with the CoupModel. Forest Ecology and Management 237 (1-3), 545–556.

Clark, I.D., Fritz, P., 1997. Environmental Isotopes in Hydrogeology. Chapman and Hall/CRC, Boca Raton.

Darling, W.G., Bath, A.H., 1988. A stable isotope study of recharge processes in the English Chalk. Journal of Hydrology 101 (1-4), 31–46.

Dreybrodt, W., 1990. The Role of Dissolution Kinetics in the Development of Karst Aquifers in Limestone: A Model Simulation of Karst Evolution. The Journal of Geology 98 (5), 639–655.

Eichler, R., 1966. Deuterium-Isotopengeochemie des Grund- und Oberflächenwassers. Geol Rundsch 55 (1), 144–159.

Feddes, R.A., Kowalik, P.J., Zaradny, H., 1978. Simulation of field water use and crop yield. Simulation monographs. Centre for Agricultural Publishing and Documentation, Wageningen.

Fenicia, F., McDonnell, J.J., Savenije, H.H.G., 2008. Learning from model improvement: On the contribution of complementary data to process understanding. Water Resour. Res. 44 (6).

Ford, D., Williams, P.D., 2013. Karst hydrogeology and geomorphology. John Wiley & Sons.

Garvelmann, J., Warscher, M., Leonhardt, G., Franz, H., Lotz, A., Kunstmann, H., 2017. Quantification and characterization of the dynamics of spring and stream water systems in the Berchtesgaden Alps with a long-term stable isotope dataset. Environ Earth Sci 76 (22), 1–17.

Gehrels, J.C., Peeters, J.E.M., Vries, J.J. de, Dekkers, M., 1998. The mechanism of soil water movement as inferred from 18 O stable isotope studies. Hydrological Sciences Journal 43 (4), 579–594.

Goldscheider, N., Drew, D., 2007. Methods in karst hydrogeology. Taylor & Francis, London.

Gribb, M.M., Forkutsa, I., Hansen, A., Chandler, D.G., McNamara, J.P., 2009. The Effect of Various Soil Hydraulic Property Estimates on Soil Moisture Simulations. Vadose Zone Journal 8 (2), 321–331.

Gupta, H.V., Kling, H., Yilmaz, K.K., Martinez, G.F., 2009. Decomposition of the mean squared error and NSE performance criteria: Implications for improving hydrological modelling. Journal of Hydrology 377 (1-2), 80–91.

Hargreaves, G.H., 1973. Estimation of Potential and Crop Evapotranspiration. Transactions of the ASAE 17 (4), 701–704. https://www.researchgate.net/profile/muhammadreza_tabatabaei/post/crop_yield_and_et_projection/attachment/59d6567679197b80779ad3d7/as%3a530360385499136%401501345917186/download/21.pdf.

Hartmann, A., Baker, A., 2017. Modelling karst vadose zone hydrology and its relevance for paleoclimate reconstruction. Earth-Science Reviews 172, 178–192.

Hartmann, A., Kralik, M., Humer, F., Lange, J., Weiler, M., 2012. Identification of a karst system's intrinsic hydrodynamic parameters: upscaling from single springs to the whole aquifer. Environ Earth Sci 65 (8), 2377–2389.

Hendry, M.J., Schmeling, E., Wassenaar, L.I., Barbour, S.L., Pratt, D., 2015. Determining the stable isotope composition of pore water from saturated and unsaturated zone core: improvements to the direct vapour equilibration laser spectrometry method. Hydrol. Earth Syst. Sci. 19 (11), 4427–4440. https://hess.copernicus.org/articles/19/4427/2015/.

Jarvis, N.J., 1989. A simple empirical model of root water uptake. Journal of Hydrology 107 (1-4), 57–72.

Klimchouk, A., 1995. Karst morphogenesis in the epikarstic zone. Cave and Karst Science 21 (2), 45–50.

Kling, H., Fuchs, M., Paulin, M., 2012. Runoff conditions in the upper Danube basin under an ensemble of climate change scenarios. Journal of Hydrology 424-425, 264–277.

Knoben, W.J.M., Freer, J.E., Woods, R.A., 2019. Technical note: Inherent benchmark or not? Comparing Nash–Sutcliffe and Kling–Gupta efficiency scores. Hydrol. Earth Syst. Sci. 23 (10), 4323–4331. https://hess.copernicus.org/articles/23/4323/2019/.

Kool, J.B., Parker, J.C., van Genuchten, M.T., 1985. Determining Soil Hydraulic Properties from One-step Outflow Experiments by Parameter Estimation: I. Theory and Numerical Studies. Soil Science Society of America Journal 49 (6), 1348–1354.

Kraller, G., 2011. Effect of Alpine karst on the hydrology of the Berchtesgadener Ache basin: a comprehensive summary of karst research in the Berchtesgaden Alps. ecomont 3 (1), 19–28.

Kuczera, G., Mroczkowski, M., 1998. Assessment of hydrologic parameter uncertainty and the worth of multiresponse data. Water Resour. Res. 34 (6), 1481–1489.

Mattei, A., Goblet, P., Barbecot, F., Guillon, S., Coquet, Y., Wang, S., 2020. Can Soil Hydraulic Parameters be Estimated from the Stable Isotope Composition of Pore Water from a Single Soil Profile? Water 12 (2), 393.

Met Office, 2006a. MIDAS: Global Radiation Observations. NCAS British Atmospheric Data Centre. https://catalogue.ceda.ac.uk/uuid/b4c028814a666a651f52f2b37a97c7c7. Accessed October 22, 2020.

Met Office, 2006b. MIDAS: UK Mean Wind Data. NCAS British Atmospheric Data Centre. https://catalogue.ceda.ac.uk/uuid/a1f65a362c26c9fa667d98c431a1ad38. Accessed October 22, 2020.

Metropolis, N., Ulam, S., 1949. The Monte Carlo method. Journal of the American Statistical Association 44 (247), 335–341.

Mishra, S., Parker, J.C., 1989. Parameter estimation for coupled unsaturated flow and transport. Water Resour. Res. 25 (3), 385–396.

Mualem, Y., 1976. A new model for predicting the hydraulic conductivity of unsaturated porous media. Water Resour. Res. 12 (3), 513–522.

Peel, M.C., Finlayson, B.L., McMahon, T.A., 2007. Updated world map of the Köppen-Geiger climate classification. Hydrol. Earth Syst. Sci. 11 (5), 1633–1644.

Rahman, M., Rosolem, R., 2017. Towards a simple representation of chalk hydrology in land surface modelling. Hydrol. Earth Syst. Sci. 21 (1), 459–471. https://hess.copernicus.org/articles/21/459/2017/.

Ries, F., Lange, J., Schmidt, S., Puhlmann, H., Sauter, M., 2015. Recharge estimation and soil moisture dynamics in a Mediterranean, semi-arid karst region. Hydrol. Earth Syst. Sci. 19 (3), 1439–1456.

Ritchie, J.T., 1972. Model for predicting evaporation from a row crop with incomplete cover. Water Resour. Res. 8 (5), 1204–1213.

Ritter, A., Hupet, F., Muñoz-Carpena, R., Lambot, S., Vanclooster, M., 2003. Using inverse methods for estimating soil hydraulic properties from field data as an alternative to direct methods. Agricultural Water Management 59 (2), 77–96.

Russo, D., Bresler, E., Shani, U., Parker, J.C., 1991. Analyses of infiltration events in relation to determining soil hydraulic properties by inverse problem methodology. Water Resour. Res. 27 (6), 1361–1373.

Seeger, S., Weiler, M., 2014. Reevaluation of transit time distributions, mean transit times and their relation to catchment topography. Hydrol. Earth Syst. Sci. 18 (12), 4751–4771. https://hess.copernicus.org/articles/18/4751/2014/.

Šimůnek, J., van Genuchten, M.T., Šejna, M., 2008. Development and Applications of the HYDRUS and STANMOD Software Packages and Related Codes. Vadose Zone Journal 7 (2), 587–600.

Sprenger, M., Herbstritt, B., Weiler, M., 2015a. Established methods and new opportunities for pore water stable isotope analysis. Hydrol. Process. 29 (25), 5174–5192.

Sprenger, M., Volkmann, T.H.M., Blume, T., Weiler, M., 2015b. Estimating flow and transport parameters in the unsaturated zone with pore water stable isotopes. Hydrol. Earth Syst. Sci. 19 (6), 2617–2635.

Strasser, U., Marke, T., 2010. ESCIMO.spread – a spreadsheet-based point snow surface energy balance model to calculate hourly snow water equivalent and melt rates for historical and changing climate conditions. Geosci. Model Dev. 3 (2), 643–652. https://gmd.copernicus.org/articles/3/643/2010/.

Stumpp, C., Stichler, W., Kandolf, M., Šimůnek, J., 2012. Effects of Land Cover and Fertilization Method on Water Flow and Solute Transport in Five Lysimeters: A Long-Term Study Using Stable Water Isotopes. Vadose Zone Journal 11 (1). https://acsess.onlinelibrary.wiley.com/doi/pdf/10.2136/vzj2011.0075?casa_token=BFjljQbtfvsAAAAA:ZEs0LsD0SlvS_A90aZMTk1r6nuDjft1ZT53l4K_d5z1JG9CehOSOnB4al1hP5r_gWLEqb3Unay755cQB.

Thomas, E.M., Lin, H., Duffy, C.J., Sullivan, P.L., Holmes, G.H., Brantley, S.L., Jin, L., 2013. Spatiotemporal Patterns of Water Stable Isotope Compositions at the Shale Hills Critical Zone Observatory: Linkages to Subsurface Hydrologic Processes. Vadose Zone Journal 12 (4), vzj2013.01.0029.

Trček, B., 2007. How can the epikarst zone influence the karst aquifer hydraulic behaviour? Environ Geol 51 (5), 761–765.

Umweltbundesamt, 2020. H2O Fachdatenbank. Version 6.0.0; Isotopen; IN50000040 Golling. https://wasser.umweltbundesamt.at/h2odb/fivestep/abfrageQdPublic.xhtml. Accessed December 15, 2020.

van Genuchten, M.T., 1980. A Closed-form Equation for Predicting the Hydraulic Conductivity of Unsaturated Soils. Soil Science Society of America Journal 44 (5), 892–898.

Vanderborght, J., Vereecken, H., 2007. Review of Dispersivities for Transport Modeling in Soils. Vadose Zone Journal 6 (1), 29–52.

Vereecken, H., Weynants, M., Javaux, M., Pachepsky, Y., Schaap, M.G., van Genuchten, M.T., 2010. Using Pedotransfer Functions to Estimate the van Genuchten-Mualem Soil Hydraulic Properties: A Review. Vadose Zone Journal 9 (4), 795–820.

Wada, Y., van Beek, L.P.H., van Kempen, C.M., Reckman, J.W.T.M., Vasak, S., Bierkens, M.F.P., 2010. Global depletion of groundwater resources. Geophys. Res. Lett. 37 (20), n/a-n/a.

Wassenaar, L.I., Hendry, M.J., Chostner, V.L., Lis, G.P., 2008. High resolution pore water delta2H and delta18O measurements by H2O(liquid)-H2O(vapor) equilibration laser spectroscopy. Environmental science & technology 42 (24), 9262–9267.

Wesseling, J.G., 1991. Meerjarige simulatie van grondwaterstroming voor verschillende bodemprofielen, grondwatertrappen en gewassen met het model SWATRE. Report 152. Winand Staring, Wageningen, the Netherlands.

Wheater, H.S., Peach, D., Binley, A., 2007. Characterising groundwater-dominated lowland catchments: the UK Lowland Catchment Research Programme (LOCAR). Hydrol. Earth Syst. Sci. 11 (1), 108–124. https://hess.copernicus.org/articles/11/108/2007/.

Williams, P., 2008. The role of the epikarst in karst and cave hydrogeology: a review. IJS 37 (1), 1–10. https://scholarcommons.usf.edu/ijs/vol37/iss1/1.

Williams, P.W., 1983. The role of the subcutaneous zone in karst hydrology. Journal of Hydrology 61 (1-3), 45–67. https://www.sciencedirect.com/science/article/pii/0022169483902342.

Zhou, J., Cheng, G., Li, X., Hu, B.X., Wang, G., 2012. Numerical Modeling of Wheat Irrigation using Coupled HYDRUS and WOFOST Models. Soil Science Society of America Journal 76 (2), 648–662.

Ehrenwörtliche Erklärung

Hiermit erkläre ich, dass die Arbeit selbständig und nur unter Verwendung der angegebenen Hilfsmittel angefertigt wurde.

Freiburg i. Br., 26. Februar 2021

Björn Kirste